Molecular Pharmacology Fast Forward. Published on December 27, 2018 as DOI: 10.1124/mol.118.114082
This article has not been copyedited and formatted. The final version may differ from this version.

Molecular basis of action of a small molecule positive allosteric modulator (PAM)-agonist at the type 1 cholecystokinin holoreceptor

Aditya J. Desai, Ingrid Mechin, Karthigeyan Nagarajan, Celine Valant, Denise Wootten, Polo C.H. Lam, Andrew Orry, Ruben Abagyan, Anil Nair, Patrick M. Sexton, Arthur Christopoulos, Laurence J. Miller

Department of Molecular Pharmacology and Experimental Therapeutics, Mayo Clinic, Scottsdale, AZ 85259 (A.J.D., L.J.M.)

In silico Drug Discovery Department, Icagen Inc. Tucson Innovation Center, Oro Valley, AZ 85755 (I.M, K.N., A.N.)

Drug Discovery Biology Theme, Monash Institute of Pharmaceutical Sciences and Department of Pharmacology, Monash University, Parkville 3052, Australia (C.V., D.W., P.M.S., A.C., L.J.M.)

Molsoft LLC, La Jolla, CA 92037 (P.C.H.L., A.O., R.A.)

Skaggs School of Pharmacy and Pharmaceutical Sciences, University of California, San Diego, La Jolla, CA 92037 (R.A.)

School of Pharmacy, Fudan University, Shanghai 201203, China (P.M.S.)

Molecular Pharmacology Fast Forward. Published on December 27, 2018 as DOI: 10.1124/mol.118.114082
This article has not been copyedited and formatted. The final version may differ from this version.

Running title: CCK receptor PAM-agonist

Address for correspondence:

Laurence J. Miller, M.D.
Mayo Clinic
13400 East Shea Blvd, Scottsdale, AZ 85259
Tel.: (480) 301-4217
Fax: (480) 301-8387
E-mail: miller@mayo.edu

Number of text pages: 40

Number of figures: 13

Number of references: 66

Words in Abstract: 216

Words Introduction: 706

Words Discussion: 1352

ABREVIATIONS: BDZ-1, (S)-1-(3-iodophenyl)-3-(1-methyl-2-oxo-5-phenyl-2,3-dihydro-1H-benzo[e][1,4]diazepin-3-yl)urea); BDZ-2, (R)-1-(3-iodophenyl)-3-(1-methyl-2-oxo-5-phenyl-2,3-dihydro-1H-benzo[e][1,4] diazepin-3-yl)urea); CCK, cholecystokinin; CCK1R or CCK2R, type 1 or 2 CCK receptor; CHO, Chinese hamster ovary; ECL, extracellular domain; ICM, internal coordinate mechanics; KRH, Krebs-Ringer-HEPES; PAM, positive allosteric modulator; TM, transmembrane domain.

Molecular Pharmacology Fast Forward. Published on December 27, 2018 as DOI: 10.1124/mol.118.114082
This article has not been copyedited and formatted. The final version may differ from this version.

ABSTRACT

Allosteric modulation of receptors provides mechanistic safety while effectively achieving biological endpoints otherwise difficult or impossible to obtain by other means. The theoretical case has been made for the development of a positive allosteric modulator (PAM) of the type 1 cholecystokinin receptor (CCK1R) having minimal intrinsic agonist activity to enhance meal-induced satiety for the treatment of obesity, while reducing the risk of side effects and/or toxicity. Unfortunately, such a drug does not currently exist. In this work, we have identified a PAM-agonist of the CCK1R, SR146131, and determined its putative binding mode and receptor activation mechanism by combining molecular modeling, chimeric CCK1R/CCK2R constructs, and site-directed mutagenesis. We probed the structure-activity relationship of analogs of SR146131 for impact on agonism versus cooperativity of the analogs. This identified structural features that might be responsible for binding affinity and potency while retaining PAM activity. SR146131 and several of its analogs were docked into the receptor structure, which had the natural endogenous peptide agonist, CCK, already in the bound state (by docking), providing a refined structural model of the intact CCK1R holoreceptor. Both SR146131 and its analogs exhibited unique probe-dependent cooperativity with orthosteric peptide agonists and were simultaneously accommodated in this model, consistent with the derived structure-activity relationships. This provides improved understanding of the molecular basis for CCK1R-directed drug development.

Introduction

Cholecystokinin (CCK) has multiple important physiologic functions, including stimulating gallbladder contraction and pancreatic exocrine secretion, regulating gastrointestinal transit, and inducing satiety in response to ingestion of a meal. Indeed, the satiety effect of CCK, mediated by the type 1 CCK receptor (CCK1R), has been demonstrated in both animal models (Chaudhri et al., 2008; Gibbs et al., 1973) and humans (Kissileff et al., 1981), supporting this receptor as a possible target for the treatment of obesity. Substantial efforts to develop small molecule agonists of the CCK1R have been undertaken by major pharmaceutical companies (Aquino et al., 1996; Berger et al., 2008; Elliott et al., 2010), however none of the agents have advanced beyond Phase II clinical trials. These efforts have been hampered by on-target side effects of potent and longer duration agonists, with lower potency agents having insufficient efficacy. A robust therapeutic window is particularly important because of the anticipated scale and duration of use.

A possible strategy to circumvent the safety and tolerability concerns is the development of a pure positive allosteric modulator (PAM) of the CCK1R that is devoid of intrinsic agonist activity (Desai et al., 2015a; Desai et al., 2016a; Desai et al., 2016b; Desai et al., 2015b; Miller and Desai, 2016). Such an agent would bind to the receptor at an allosteric site that is distinct from the natural orthosteric ligand binding site, allowing concurrent occupation and potentiation of biological responses to CCK. This would occur only during the limited and finite period of time when nutrients enter the duodenum to stimulate the release of endogenous hormone, resulting in amplification of the natural effects of CCK. Such a mechanism of action would be predicted to lead to an early peak in satiety, reducing meal size and contributing to body weight reduction, while, in the meantime, minimizing the side effects observed with full agonists of the CCK1R and avoiding the tolerance often experienced with such agonists.

A small molecule ligand-binding site within the CCK1R has been localized to a pocket high within the helical transmembrane domain using receptor mutagenesis, fluorescence, and photoaffinity labeling approaches (Cawston et al., 2012; Desai et al., 2015c; Hadac et al., 2006; Harikumar et al.,

2013). This pocket assumes distinct conformations conferring different molecular determinants of ligand binding in its inactive state occupied by antagonist ligands (Cawston et al., 2012), versus its active state occupied by agonist ligands (Desai et al., 2015c; Harikumar et al., 2013).

We previously proposed an experimental strategy in which a key chemical group (isopropyl), identified in small molecule structure-activity studies as critical for its agonist activity, would be changed or eliminated to reduce its intrinsic agonist activity, while theoretically stabilizing a conformation that reduces the energy barrier of activation, and possibly exhibiting PAM activity (Desai et al., 2015b). However, the first application of this strategy to GI181771X, an allosteric agonist lacking intrinsic PAM activity, was unsuccessful in achieving PAM activity, and instead resulted in a negative allosteric modulator (NAM) of CCK action (Desai et al., 2015b). We postulated that these analogs could adopt poses in the allosteric pocket that would be distinct from that of the parent compound (Desai et al., 2015b).

In the current work, we identified the small molecule ligand, SR146131 (Bignon et al., 1999), as a selective CCK1R PAM-agonist that could form a promising template for differentiation of structure-activity driving intrinsic efficacy versus allosteric enhancement. SR146131 differed from an antagonist in the same series, SR27897, possessing a cyclohexylethyl group attached to its thiazol ring, as well as two methyl groups on the indole ring and two methoxy groups on the phenyl ring (Gouldson et al., 2000). Moreover, SR146131 enhanced the potency of functional responses to the orthosteric ligand, CCK. Docking of the compound into a previously developed molecular model of CCK1R in its active state (Harikumar et al., 2013), predicted key interactions between the 5-methoxy group on the phenyl ring of SR146131 with transmembrane segment residue Leu 7.39 of CCK1R that we had previously linked to the agonist activity of GI181771X. Consequently, we studied a series of structural analogs to provide insights into the molecular basis of agonism and cooperativity.

Included in this series of compounds was an analog with attenuated agonist activity, reflected in lower binding affinity, which retained its positive cooperativity on CCK action. This ligand was docked into a refined molecular model that accommodated simultaneous binding of natural CCK

Molecular Pharmacology Fast Forward. Published on December 27, 2018 as DOI: 10.1124/mol.118.114082
This article has not been copyedited and formatted. The final version may differ from this version.

peptide. Within the compound series, the PAM activity was correlated with its intrinsic efficacy, thus identifying structural features for binding affinity independent of efficacy and allosteric modulation. While future work will focus on the potential to separate intrinsic efficacy and positive modulation, the current study advances our understanding of the molecular determinants for modulator binding that may be useful in the design and development of ligands with tailored molecular properties.

Molecular Pharmacology Fast Forward. Published on December 27, 2018 as DOI: 10.1124/mol.118.114082
This article has not been copyedited and formatted. The final version may differ from this version.

Materials and Methods

Materials. Ham's F-12 medium, OptiMEM medium, L-glutamine, Lipofectamine LTX and PLUS reagents were from Invitrogen (Carlsbad, CA). Quest Fluo-8-AM was from AAT Bioquest Inc. (Sunnyvale, CA). Fetal Clone II tissue culture medium supplement was from Hyclone Laboratories (Logan, UT). Microscint, Unifilter 96-well microplates with bonded GF/B filters were from PerkinElmer Life and Analytical Sciences (Shallon, CT). Costar 96-well V bottom assay plates and the black assay plates with clear bottoms were from Corning (Corning, NY). All other reagents were analytical grade.

Ligands. SR146131, 2-[4-(4-chloro-2,5-dimethoxyphenyl)-5-(2-cyclohexyl-ethyl)-thiazol-2-ylcarbam-oyl]-5,7-dimethyl-indol-1-yl-1-acetic acid, was provided by Sanofi (structure shown in Fig. 1A). This ligand is a potent full agonist at the CCK1R (Bignon et al., 1999; Gouldson et al., 2000). Cholecystokinin octapeptide (CCK-26-33, based on the numbering of CCK-33; also known as CCK-8 and commonly identified as CCK) was purchased from Peninsula Laboratories (Belmont, CA). The O-phenylethyl ester analog of CCK previously demonstrated to be a partial agonist at the CCK1R (CCK-OPE) (Gaisano et al., 1989) was synthesized in our laboratory. The CCK1R-selective 1,4-benzodiazepine radioligand (^{125}I-BDZ-1, (S)-1-(3-iodophenyl)-3-(1-methyl-2-oxo-5-phenyl-2,3-dihydro-1H-benzo[e][1,4]diazepin-3-yl)urea) and the CCK2R-selective radioligand (^{125}I-BDZ-2, (R)-1-(3-iodophenyl)-3-(1-methyl-2-oxo-5-phenyl-2,3-dihydro-1H-benzo[e][1,4] diazepin-3-yl)urea) were prepared as we described previously (Akgun et al., 2009). These were radioiodinated using oxidative techniques with iodobeads (Pearce, Rockford, IL), and the products were purified to homogeneity on reversed-phase HPLC (Powers et al., 1988). Both radioligands had specific radioactivities of approximately 2000 Ci/mmol.

CCK Receptor-Bearing Cell Lines and Membrane Preparation. Chinese Hamster Ovary (CHO) cell lines stably expressing a series of CCK receptor constructs that have been previously characterized (Cawston et al., 2012; Desai et al., 2015b; Harikumar et al., 2013) were utilized in the current studies. The cell lines were passaged approximately two times per week, and were maintained

Molecular Pharmacology Fast Forward. Published on December 27, 2018 as DOI: 10.1124/mol.118.114082
This article has not been copyedited and formatted. The final version may differ from this version.

at 37°C in Ham's F-12 medium supplemented with 5% Fetal Clone II in a humidified environment containing 5% carbon dioxide. As described previously (Hadac et al., 1996), receptor-bearing membrane fractions were prepared using homogenization and sucrose-density gradient centrifugation, with the resulting particulate fraction suspended in Krebs-Ringer-HEPES (KRH) medium (in mM, 25 HEPES, pH 7.4, 104 NaCl, 5 KCl, 1.5 $CaCl_2$, 1.0 KH_2PO_4, 1.2 $MgSO_4$, 1.2 $MgCl_2$) containing 0.01% soybean trypsin inhibitor and 1 mM phenylmethylsulfonyl fluoride and stored at -80°C until use.

Receptor Binding Assays. Individual radioligand competition-binding assays were performed in duplicate using benzodiazepine radioligands (Cawston et al., 2012; Desai et al., 2015b; Harikumar et al., 2013). Briefly, ~5-7 μg membranes were added to a 100 μl assay volume in a clear 96-well plate containing increasing concentrations of SR146131 and ~20-25 pM radioligand, in KRH medium and incubated for 60 min at room temperature. The reaction was then terminated by vacuum filtration using Unifilter-96 well microplates with bonded GF/B filters in a Filtermate Harvester (PerkinElmer, Waltham, MA). Non-saturable binding was determined using the corresponding unlabeled ligand, 1 μM BDZ-1 or BDZ-2. The plates were washed six times using 0.9% NaCl and 0.2% bovine serum albumin and then dried, with radioactivity quantified using a Top CountNXT™ instrument (Packard, Meriden, CT) after addition of 30 μl Microscint.

Intracellular Calcium Assays. CCK receptor-mediated biological responses were measured by quantifying intracellular calcium increases in response to SR146131 (Desai et al., 2014; Desai et al., 2015b). Briefly, cells were seeded in sterile clear-bottom black 96-well tissue culture plates 24 h before the assay to achieve 75-80 percent confluence at the time of the assays. Cells were loaded with 0.75 μM Fluo 8 AM dye in KRH medium containing 2.5 mM probenecid for 45 min at 37°C in the dark. They were washed once and the assay was performed in a Flexstation 3.0 plate reader (Molecular Devices, Sunnyvale, CA) using robotic addition of the appropriate agonist ligand. Intracellular calcium responses were quantified by measuring fluorescence emission intensity at 525 nm after excitation at 485 nm, with data collection every 4 sec over a 120 sec period, while maintaining a constant temperature of 37°C. Concentration-response curves were constructed by plotting the peak responses. To test their positive allosteric effect, fixed concentrations of compounds

were added simultaneously with increasing concentrations of CCK, or the partial agonist, CCK-OPE that is a phenethyl ester analog of CCK (Gaisano et al., 1989), and intracellular calcium measurements were taken as mentioned above.

Molecular Modeling. SR146131, together with 159 known CCK1R agonists and 1739 other CCK1R ligands (not identified as agonists) collected from ChEMBL_15, were docked to the previously-generated CCK1R agonist receptor models (Desai et al., 2015c; Harikumar et al., 2013) using MolSoft ICM 3.8 (Totrov and Abagyan, 1997). The best agonist receptor model achieved an area under ROC curve (AUC) value of 87%, effectively differentiating the agonists from other ligands. We clustered the docking poses of all agonists using the ICM atomic property field (APF) method (Totrov, 2008) with a distance cutoff of 0.4. The majority of the CCK1R agonists docked into two distinct docking pose families, consistent with their chemotype (benzodiazepine core: 67 members; piperazine core: 64 members), indicating the general applicability and consistency of the receptor model for docking. SR146131 achieved an ICM docking score of -39, more favorable than the ICM docking score of -32 for a typical binder.

We also developed a refined CCK1R homology model using the recently solved structure of the orexin-1 receptor in complex with the selective antagonist SB-674042 (PDB code: 4ZJ8) (Yin et al., 2016) as a template, since this receptor is closer in sequence to CCK1R than the A2a adenosine receptor used in our previous CCK1R model. The orexin-1 receptor has 33% sequence identity/53% homology with CCK1R, versus 26% sequence identity/42% homology for the A2a adenosine receptor. Although 4ZJ8 is in an antagonist-bound conformation, it also offers the advantage of presenting a pre-formed ligand binding site. The starting homology model was generated using Prime (Jacobson et al., 2004) after multiple sequence alignment of several human and mouse class A GPCR sequences. The NMR structure of the amino terminus of CCK1R (PDB code: 1D6G (Pellegrini and Mierke, 1999)) was then grafted to the core helical bundle domain. Extracellular loops for the new model were sampled using Loop Modeler from MOE (Labute, 2010) and the N-amino terminus was sampled by Macromodel (Watts et al., 2014). From the numerous N-amino termini and loop combinations obtained, we retained and minimized those in agreement with previously reported

experimental data (Ding et al., 2001; Ding et al., 2002; Dong et al., 2009; Gigoux et al., 1998; Gigoux et al., 1999; Giragossian and Mierke, 2001; Hadac et al., 1998; Ji et al., 1997; Kennedy et al., 1997) and without substantial clashes.

We performed induced-fit docking of the CCK peptide in the best new model (out of several prioritized models), taking into account the mutational data and the reported potency/efficacy of peptide on the CCK1R mutants (Ding et al., 2002; Gigoux et al., 1998; Gigoux et al., 1999), intermolecular Nuclear Overhauser Effects (NOEs) observed between CCK and the receptor (Giragossian and Mierke, 2001; Kennedy et al., 1997), as well as photoaffinity labeling data (Ding et al., 2001; Dong et al., 2009; Hadac et al., 1998; Ji et al., 1997). These considerations are reviewed in Supplemental Table 1. The CCK1R-CCK peptide complex structure was subsequently used to dock SR146131.

The three-molecule complex (CCK1R + CCK peptide + SR146131) was then subjected to 1 μs molecular dynamics simulation using Desmond (Bowers et al., 2006) after placing a POPC membrane system and addition of explicit solvent, TIP3P water system together with Cl- ions to neutralize the system. In addition, 0.15M NaCl salt was also added to the system. The transmembrane segments annotated in the Uniprot entry for CCK1R were used for the placement of the POPC bilayer. Twenty-six frames from the simulation were selected at even intervals of 40 ns, starting at the initial frame, for docking of compound 12 using Glide (Schrödinger LLC., USA) (Friesner et al., 2004) without any constraints. A maximum of six poses was retained for each docking, and only those poses with a docking score better than -9.0 were subjected to binding mode analysis. For these poses, we observed a binding mode where the acid group of compound 12 interacts with Arg 6.58 about 42% of the time and the same group interacts with Asn 6.55 for about 24% of the time. We also found that Tyr 4.63 interacts with the same acid group in a substantial number (33%) of binding poses, either as sole partner or in addition to Asn 6.55. We also observed in a small number (6%) of cases some interactions with Tyr 4.60.

Molecular Pharmacology Fast Forward. Published on December 27, 2018 as DOI: 10.1124/mol.118.114082
This article has not been copyedited and formatted. The final version may differ from this version.

There is strong mutational data supporting the critical roles of Arg 6.58 and Asn 6.55 in SR146131 binding (Gouldson et al., 2000 and Escrieut et al., 2002), so we decided to focus on these residues for further analysis. Supplemental Table 2 summarizes the data describing the functional impact of CCK1R mutations on SR146131 action, and the ligand-receptor residue distances in our models. Two representative frames, each leading consistently to one of these two binding modes, were selected and used as starting points for docking of SR146131 and its analogs using Glide. Here also, no constraints were employed for docking of these compounds to the CCK peptide-bound receptor structure. The top poses for docked SR146131 and its analogs were then submitted to Prime-mmGBSA calculations (Sherman et al., 2006). This was used to refine ranking based on relative binding affinities (ΔG) and to evaluate structural changes on the receptor occurring after binding of this series of ligands, both in the presence and absence of the CCK peptide. Our models differ from all previously-described molecular models of this receptor since they simultaneously accommodate binding of both the CCK peptide and a small molecule ligand, here SR146131 and its analogs. This also may be helpful in understanding subtle differences in the functional behavior of different ligands.

Data Analysis and Statistics. All data were analyzed using Prism 6 or 7 (GraphPad Software, Inc., San Diego, CA). In all analyses, the data were unweighted, with the mean of replicates in each experiment considered as an individual point. Throughout the manuscript, data are presented as the mean of these values ± S.E.M. with the number of replicates of independent experiments noted. Concentration-response data were analyzed using the three-parameter logistic equation (May et al., 2007), $E = Bottom + (Top-Bottom)[A]/[A]+[EC_{50}]$, where Bottom represents the E value in the absence of ligand, Top represents the maximal stimulation in the presence of ligand, [A] is the molar concentration of ligand, and EC_{50} represents the molar concentration of ligand required to generate a response halfway between Top and Bottom. The competitive model was utilized for the analysis of the binding data, with data corrected for radioligand occupancy using the Cheng-Prusoff equation (Cheng and Prusoff, 1973). Differences in receptor binding and signalling parameters between various constructs were statistically evaluated using one way ANOVA with Dunnett's multiple comparison post-test, with $p<0.05$ considered to be statistically significant.

Molecular Pharmacology Fast Forward. Published on December 27, 2018 as DOI: 10.1124/mol.118.114082
This article has not been copyedited and formatted. The final version may differ from this version.

Radioligand equilibrium binding curves with allosteric ligands were fitted to either a one-site inhibition mass action curve to determine inhibitor potency (IC_{50}) estimates, which were then converted to K_i values as appropriate, or an allosteric ternary complex model (Eq. 1) to derive estimates of allosteric modulator affinity (K_B) and cooperativity between the compound and radioligand (α); where α>1 denotes positive cooperativity, 0<α<1 denotes negative cooperativity and α=1 denotes neutral cooperativity (Christopoulos and Kenakin, 2002; Ehlert, 1988).

Eq. 1

$$E = \frac{B_{max}[A]}{[A] + (K_A)\left(\frac{K_B + [B]}{K_B + \alpha[B]}\right)}$$

where K_A and K_B represent the equilibrium dissociation constant of the radioligand and interacting ligand, respectively, and [A] and [B] denote their concentrations. B_{max} is the maximum number of binding sites on the cell. Dissociation kinetic data were fit to a one-phase exponential decay function to derive the apparent rate constant of dissociation (K_{off}) in the absence or presence of each compound.

Functional studies for the interaction of orthosteric agonist and allosteric modulator was either fitted to a three parameter logistic equation or an operational model of allosterism and agonism (Leach et al., 2007) (Eq. 2) to derive estimates of affinity and combined binding/efficacy cooperativity:

Eq. 2

$$E = \frac{E_m(\tau_A[A](K_B + \alpha\beta[B]) + \tau_B[B]K_A)^n}{([A]K_B + K_AK_B + K_A[B] + \alpha[A][B])^n + (\tau_A[A](K_B + \alpha\beta[B] + \tau_B[B]K_A)^n}$$

where E_m is the maximum possible response for the system, [A] and [B] are the concentration of the orthosteric agonist and allosteric modulator, respectively, τ_A and τ_B are the signaling efficacy of the respective ligands, K_A and K_B is the equilibrium dissociation constant for the respective ligands, n is a transducer slope factor linking occupancy to response, α is the cooperativity factor (as described

Molecular Pharmacology Fast Forward. Published on December 27, 2018 as DOI: 10.1124/mol.118.114082
This article has not been copyedited and formatted. The final version may differ from this version.

above) and β is an empirical scaling factor describing the allosteric effect of the modulator on the orthosteric agonist signaling efficacy.

Molecular Pharmacology Fast Forward. Published on December 27, 2018 as DOI: 10.1124/mol.118.114082
This article has not been copyedited and formatted. The final version may differ from this version.

Results

Subtype Selectivity of SR14131 at Wild Type CCK Receptors. Consistent with previous reports (Bignon et al., 1999; Gouldson et al., 2000), SR146131 displayed concentration-dependent agonism, stimulating maximal intracellular calcium responses in the CCK1R-bearing CHO-CCK1R cells similar to that stimulated by natural CCK, while lacking agonism in the CCK2R-bearing CHO-CCK2R cell line over equivalent concentrations (Fig. 1B). This compound displayed high potency on CCK1R, with an EC_{50} of 43 ± 2 pM (mean ± S.E.M., n=6), and substantial functional subtype selectivity over CCK2R (Fig. 1B).

Competition-binding studies using radiolabeled non-peptidyl antagonist benzodiazepines (radioiodinated BDZ-1 and BDZ-2 for CCK1R and CCK2R, respectively), which bind to an intrahelical allosteric site (Cawston et al., 2012), were performed to assess the binding properties of SR146131 at both CCKR subtypes. SR146131 fully competed for binding of the ^{125}I-BDZ-1 at CCK1R, yielding a pK_i of 8.30 ± 0.09 (n=6) using a competitive binding model (Fig. 1C), whereas it displayed incomplete inhibition (~50%) of the saturable binding of ^{125}I-BDZ-2 at CCK2R (n=4) (Fig. 1C), indicative of an allosteric mode of interaction between the two ligands. We recently demonstrated that similar behavior of another CCK receptor ligand was due to interactions across a receptor homodimer, and this is likely also true for the SR146131 compound (Desai et al., 2015c). To account for the allosteric nature of the binding, these data were subsequently analyzed using an allosteric ternary complex model (Christopoulos and Kenakin, 2002). The derived constant for SR146131 binding to the free CCK1R (pK_B) was 8.24 ± 0.08 (n=5), and this was different from that at CCK2R (7.20 ± 0.17, n=4, $p < 0.05$, unpaired t-test). The cooperativity constants with the iodinated radioligand, Log α_{BDZ-1} or Log α_{BDZ-2}, were also lower at CCK1R than at the CCK2R, respectively (-1.22 ± 0.10 vs. -0.36 ± 0.07, $p < 0.05$, unpaired t-test) indicating stronger negative cooperativity at the CCK1R compared to CCK2R.

Allosteric Action of SR146131 at CHO-CCK1R cells. We examined possible PAM activity of SR146131 by measuring dose-response curves of both CCK and a phenethyl ester analog of CCK

(CCK-OPE), which is a partial agonist at the CCK1R, in CHO-CCK1R cells in the absence or presence of increasing concentrations of SR146131. These analyses confirmed that SR146131 is a PAM-agonist since it potentiated both CCK- and CCK-OPE-dependent intracellular calcium mobilization (Fig. 2A-B). The strong intrinsic agonism of SR146131 makes it difficult to apply operational models to quantify the degree of allosteric modulation, since a maximal system response is reached at concentrations much lower than the predicted pK_B of SR146131. In these interaction studies, low concentrations of SR146131 were used, and these data were analyzed with the operational model of allosterism by fixing the pK_B to the affinity of SR146131 defined in radioligand binding to yield composite (affinity and efficacy) cooperativity estimates. One caveat with fixing the pK_B in this analysis is that the assay conditions for radioligand binding (equilibrium conditions and performed in membranes) and the functional assay (non-equilibrium and performed in whole cells) are not equivalent. Since the estimated pK_B can differ under different experimental conditions, and pK_B and alpha are linked in the operational analysis, under/over estimation of this value can influence the derived cooperativity estimates. Nonetheless, this analysis confirmed the high intrinsic agonist efficacy of SR146131 with consistent efficacies predicted from both data sets with operational Log τ_B values of 2.41 ± 0.06 (τ_B = 263) derived from the CCK interaction curve and 2.32 ± 0.11 (τ_B = 209) from the CCK-OPE analysis. Consistent with visual observation of the data, cooperativity estimates from this analysis predict that SR146131 has greater cooperativity with CCK-OPE (Log $\alpha\beta_{CCK\text{-}OPE}$ = 3.72 ± 0.08 ($\alpha\beta_{CCK\text{-}OPE}$ = 5248)) than with CCK (Log $\alpha\beta_{CCK}$ = 2.75 ± 0.25 ($\alpha\beta_{CCK}$ = 562)).

SR146131 Function at CCK1R/CCK2R Chimeric Constructs. An experimental structure-activity relationship approach for the small molecule ligand-binding site was used to interrogate the molecular basis of ligand-receptor and/or peptide interaction of SR146131. We have previously utilized this approach for molecular understanding of the action of other CCKR small molecule antagonists (Cawston et al., 2012), and agonists (Desai et al., 2015c; Harikumar et al., 2013), using CCK1R/CCK2R constructs with exchanged intrahelical allosteric pocket residues between these receptors. Receptor density of stably expressed constructs and effect of mutation on BDZ and CCK ligand affinities have been previously reported (Cawston et al., 2012; Desai et al., 2015c; Harikumar

et al., 2013). In the first series of studies, we used receptor constructs exchanging individual TM2, TM3, TM6 and TM7 segments of CCK1R with the corresponding residues of CCK2R, as well as the converse constructs (Cawston et al., 2012; Desai et al., 2015b; Harikumar et al., 2013) (Fig. 3A, Table 1). In the case of the CCK1R-based chimeras, the TM7 construct (CCK1R L7.39H; all residue numbers are labelled according to the Ballesteros and Weinstein class A numbering scheme (Ballesteros and Weinstein, 1992)) showed greatest loss in ligand-induced intracellular calcium mobilization, followed by the TM2 construct (CCK1R N2.61T). Of note, at the TM3- and TM6-based chimeras (CCK1R T3.28V, T3.29S, and I6.51V, F6.52Y) there were small but statistically significant right-shifts in EC_{50} values. Interestingly, of the converse CCK2R-based constructs with exchanged residues of CCK1R, only the TM7 and TM6 constructs exhibited a partial gain-of-function in response to SR146131 (Fig. 3B, Table 1).

Competition-binding experiments utilizing ^{125}I-BDZ-1 or ^{125}I-BDZ-2 radioligands on the CCK receptor chimeras (Fig. 3C, Table 1) demonstrated that, in the CCK1R-based chimeras, the TM7 construct had greatest impact on binding, followed by the TM2 and TM6 constructs, whereas the TM3 construct lead to an increase in SR146131 pIC_{50} values. These data were analyzed with the operational allosteric model to yield values of pK_B and Log α for the respective radioligands, ^{125}I-BDZ-1 or ^{125}I-BDZ-2, illustrating that the chimeras impacted both affinity and binding cooperativity (Table 1). The CCK2R-based constructs exhibited the converse increase or decrease in binding inhibition, although this was only statistically significant for the TM6 and TM7 chimeras (Fig. 3D, Table 1). For the TM6 chimera the effect was primarily driven by increased negative cooperativity, while the TM7 chimera altered both affinity and cooperativity (Table 1). Of note, as reported in our previous studies (Cawston et al., 2012; Harikumar et al., 2013), the CCK2R TM2 chimera showed a complete loss of binding of ^{125}I-BDZ-2 and hence could not be assessed. Overall, these data suggested a greater importance of residues constituting the CCK1R TM7 (Leu 7.39) and TM2 (Asn 2.61) constructs in docking of SR146131.

Modeling and Docking of SR146131 in the CCK1R Helical Bundle. SR146131 was initially docked into our previously reported model of the active conformation of the helical bundle of

CCK1R (Harikumar et al., 2013) (Fig. 4). The best-fitting, most energetically favorable model predicted that the compound docked within the same intramembranous intrahelical pocket of the CCK1R previously predicted for GI181771X (Harikumar et al., 2013), with the thiazole ring of SR146131 and the benzodiazepine ring of GI181771X occupying the same space (Fig. 4, 5). The main difference in these models is that GI181771X makes closer interactions with TM6, including two hydrogen bonds with Asn 6.55 and Arg 6.58 (Fig. 5B). The pocket occupied by SR146131 was formed by TM2, TM3, TM6 and TM7, with the indole ring oriented toward the extracellular region and the carboxylate group facing TM6 and making interactions with Asn 6.55. This model predicted that the residues Met 3.32, Val 3.36 and Trp 6.48 formed the steric bulk lining the bottom of the pocket. Residues Asn 2.61 and Asn 2.65 and Tyr 7.43 formed a hydrogen-bonding network connecting TM2 and TM7 (Fig. 4, 5). Furthermore, Ser 7.42 formed two intrahelical hydrogen bonds with the backbone of TM7 (Fig. 4, 5A).

As noted earlier, the agonist SR146131 and the closely-related antagonist SR27897 differ by the presence of two methyl groups on the indole ring, an additional cyclohexylethyl group attached to the thiazol ring, and two methoxy groups on the phenyl ring of SR146131 (Gouldson et al., 2000). Since the two methyl groups on the indole ring are predicted to face the extracellular surface, they are unlikely to contribute any molecular interaction important for agonist activity. In contrast, the cyclohexylethyl group and the phenyl ring are predicted to bind deep inside the pocket (Fig. 4, 5). According to this model, the cyclohexylethyl group is predicted to point toward the pocket formed by TM3, TM5, and TM6 to make key interactions with Val 3.36 (contact area 21 $Å^2$), Trp 6.48 (17 $Å^2$), and Phe 6.52, and the phenyl ring is accommodated in the hydrophobic pocket formed by TM2, TM3, and TM7. This model predicts important interactions of the methoxy groups on the phenyl ring with residues Thr 3.29 and Leu 7.39 that were important for SR146131 function as observed in the CCK1R/CCK2R chimeric receptor data. The model also predicts that the 2-methoxy group interacts with Thr 3.29, Tyr 3.30, and Met 3.32 (40 $Å^2$), and the 5-methoxy group can interact with Leu 7.39, Ser 7.42, Asn 2.61, and Met 3.32 (Fig. 4, 5A).

Characterization of Receptor Mutants Predicted to Be Important for SR146131 Activity. Based on the proposed binding hypothesis by docking of SR146131, we identified additional receptor residues that were predicted to be in spatial proximity to the ligand, and thus could have functional importance. Of these, we used alanine-replacement mutants for Met 3.32, Val 3.36, and Trp 6.48 that were used in an earlier study (Bmax, pmol/mg: CCK1R WT, 5.0 ± 1.0; M3.32A, 151 ± 63; V3.36A, 0.9 ± 0.4; W6.48A, 0.8 ± 0.2) (Desai et al., 2015c), and also generated an alanine-replacement mutant for Ser 7.42 (Bmax, pmol/mg: 82.6 ± 12.0). Biological activity and binding parameters for SR146131 at these CCK1R constructs are reflected in Fig. 6 and Table 2. Because of the differences in levels of receptor construct expression, we include Log τ_B values normalized to levels of cell surface binding, Bmax, in Table 2 to reflect intrinsic efficacy of SR146131 at each of the receptor constructs relative to that at wild type CCK1R. This difference was statistically significant for three of the constructs, with efficacy decreased for M3.32A and increased for V3.36A, and S6.48A.

Functional Effects of Modification of SR146131. In an attempt to reduce the agonist activity of SR146131 while still maintaining its PAM activity, we utilized structurally-related compounds that were available from Sanofi with modifications on the phenyl ring that was predicted to be located at an equivalent position to the isopropyl group of GI181771X (Table 3). Of these, compounds with appreciable structural differences in this part of the molecule that retained the PAM activity included compound 2 (methyl group), compound 4 (hydrogen), and compound 12 (ethyl group) (Fig. 7). These compounds showed 1.3-, 1.3-, and 1.2-fold lower potencies than SR146131, respectively, at the CCK1R WT (Table 3). Using ^{125}I-BDZ-1 as radiolabel, IC_{50} values of compounds 2, 4, and 12 were determined to be 3.65-, 5.0-, and 32.0-times lower than SR146131, respectively (pK_i values: 7.65 ± 0.03, compound 2; 7.52 ± 0.04, compound 4; 6.70 ± 0.02, compound 12, n=3). Of note, the pIC_{50} of compound 2 was different from compound 12 ($p<0.05$; One way ANOVA, Dunnett's post-test). Application of the operational model for allosterism revealed that compound 2 and compound 4 had markedly diminished efficacy and cooperativity (compound 4 exhibiting no PAM activity), with greatest impact seen with compound 4 (compound 2, Log τ_B = 0.42, Log $\alpha\beta$ = 0.76;

Molecular Pharmacology Fast Forward. Published on December 27, 2018 as DOI: 10.1124/mol.118.114082
This article has not been copyedited and formatted. The final version may differ from this version.

compound 4, Log τ_B = 0.02, Log $\alpha\beta$ = 0.06) (Fig. 8A, B). Compound 12 was unique among these SR146131 analogs in that it retained efficacy and positive allosteric modulatory activity on CCK action that was similar to that of the parental compound (Fig. 9A), with a log τ_B value of 2.27 ± 0.04 and Log $\alpha\beta$ of 2.41 ± 0.19 ($\alpha\beta$ = 257). Of note, this effect was also seen on cells expressing 11-fold lower CCK1R WT on their surface, Log τ_B = 1.17 and Log $\alpha\beta$ = 1.41). Interestingly, like SR146131, compound 12 exhibited stronger PAM effect when using the partial agonist, CCK-OPE, as the orthosteric ligand (Fig 9B). The quantitative parameters for this effect were Log $\alpha\beta$ = 4.18 ± 0.08, and Log τ_B = 2.28 ± 0.36.

Enhanced Molecular Model for Docking of SR146131 to the CCK1R Holoreceptor. Using the available structure-function data and the new model derived from the ligand-bound orexin-1 receptor as template, we have generated several refined models of CCK1R by loop refinement, molecular dynamic simulations and ensemble dockings. Based on this, we were able to develop a model that allowed the simultaneous occupation of both CCK peptide and SR146131 or its analogs. We believe that this is the first reported CCK1R model with natural peptide ligand and a small molecule modulator ligand bound simultaneously. In these models, the two ligands reside adjacent to each other, with predicted ligand-ligand interactions that likely contribute to some of the biological behavior of the tested small molecules (Figs. 10 and 11). The synergistic effect of the peptide and the small molecule ligand binding could be deciphered by sampling of the extracellular domain and the loops, molecular dynamics simulations and mmGBSA calculations, which had not been previously exploited for this receptor. We have utilized these new models to guide interpretation of the cooperativity of both CCK peptide and the small molecule ligands. Two of these models, corresponding to docking poses of SR146131 and analogues into two representative frames from the MD simulations mentioned in the Methods section, are discussed below.

Molecular Modeling and Binding Hypothesis for SR146131 and its Analogs. Initial models of the ternary complex between CCK1R, CCK peptide and SR146131 were further subjected to molecular dynamics simulations to generate refined binding site and CCK peptide conformations for the 13 structurally-related analogs of SR146131 discussed above. Two putative binding modes for

SR146131 were observed from the molecular dynamics simulations with about the same frequency. Changes in binding mode seem driven by slight structural variations in the receptor and CCK peptide over the course of the MD simulations. We decided to investigate both binding modes in more detail and performed docking studies for all 14 compounds in both pocket conformations using Glide (Schrödinger LLC., USA) (Friesner et al., 2004). Top poses for these active compounds were consistent with the original SR146131 putative binding mode in both cases with highly negative docking scores, reinforcing our confidence in the new model. For all 14 ligands studied and in both binding modes, the thiazole ring of the small molecule ligand exhibits pi stacking with the tryptophan (Trp 30) of the CCK peptide, indicating potential direct interaction between the endogenous agonist and the small molecule ligands as a component of their cooperativity. Figures 10 and 11 exemplify the two putative binding modes for docked compound 12 by itself and in comparison to docked SR146131 and are discussed in detail below. General observations are also given for other representative analogs studied in this paper.

Binding mode 1 (Fig. 10A), where the acid group of the compounds is involved in a salt bridge with Arg 6.58, gave the best docking scores and most consistent poses for all 14 compounds. This binding mode is in reasonable agreement with most of the mutational data reported to date that has impact on the binding of SR146131 to CCK1R. This involves loss of activity of SR146131 at receptor constructs with mutations such as, C94L (Cys 2.57 to Leu), F97A (Phe 2.60 to Ala), G122L (Gly 3.33 to Leu), V125A (Val 3.36 to Ala), F198A (part of ECL2), I329A(F) (Ile 6.51 to Ala or Phe), R336A(D)(M) (Arg 6.58 to Ala or Asp or Met), and I352A (Ile 7.35 to Ala) and L356A (Leu 7.39 to Ala). All of these residues are in the close vicinity of this ligand's proposed binding site (see Fig. 10 for orientations of these residues, except Gly 3.33).

However, the effect of the N333A (Asn 6.55 to Ala) mutation to the loss of binding affinity of SR146131 to CCK1R could not be easily rationalized by this binding hypothesis, although the docked compounds are within 6.4Å of Asn 6.55. Additional induced effects and thus stronger interactions of Asn 6.55 with the ligand may be possible since this residue is within TM6, known to

exhibit considerable movement and to play important functional roles in many GPCRs (Latorraca et al., 2017; Rasmussen et al., 2011).

Binding mode 2 (Fig. 10B), when compared to binding mode 1, shows a flipped orientation of the indole moiety. In this case, the acid group of the ligand is involved in a hydrogen bond with the side chain of Asn 6.55, while the indole scaffold has a stacking interaction with the side chain of Arg 6.58. In this binding mode (Fig. 11B), we observe an additional difference between docked SR146131 and compound 12 of approximately 1 Å shift of the indole scaffold due to the additional methyl group at position 7 and the proximity of the side chain of Asn 6.55. This binding mode also corresponds to good docking scores, although less negative, and increased variability in docking poses. Due to these reasons, we prioritized binding mode 1 and the Prime-mmGBSA calculations discussed in the next section focus on binding mode 1.

The lower half of the compounds, below the amide linker, exhibits similar orientations and interactions in both binding modes, independent of the orientation of the indole moiety: Cys 2.57, Val 3.36, Trp 6.48 and Ile 6.51 are involved in hydrophobic interactions with the cyclohexyl moiety, in agreement with both new mutational data reported in this paper and historical experimental data (Gouldson et al., 2000). Detailed analysis of compound 12 binding modes 1 and 2 predict that Asn 2.61, Met 3.32 and Ser 7.42 form interactions with both the cyclohexyl and the substituted benzyl group. Phe 2.60, Asn 2.65, Phe 198, Leu 7.39 and Tyr 7.43 delimit the substituted benzene ring binding region. In addition, this new model sheds light on one potentially interesting aspect of PAM regulation: in both binding modes 1 and 2, the substituted benzene of compound 12 is near CCK peptide residue Trp 30, where they show stacking interactions (in addition to the stacking of the thiazole ring to Trp 30 within the CCK peptide observed for all representatives) (Fig. 10). Differences were observed for the interactions of benzene ring substituents to the receptor in the two models. Particularly to compound 12 vs SR146131, the substitution in position 5, (ethyl vs methoxy groups) led to differences in interaction energies with Leu 7.39 and Ser 7.42. Similar changes were seen in the interaction with Asn 2.65 with substitutions at position 4 (Cl vs methoxy).

Molecular Pharmacology Fast Forward. Published on December 27, 2018 as DOI: 10.1124/mol.118.114082
This article has not been copyedited and formatted. The final version may differ from this version.

Prime-mmGBSA Calculations for SR146131 and its Analogs in Binding Mode 1. In an attempt to better understand the effect of substitutions around SR146131 we ran Prime-mmGBSA induced-fit calculations for all compounds docked in CCK1R with previously described binding mode 1, both in the presence and absence of CCK peptide. Figure 12 highlights the differences in CCK1R conformations between bound compound 10 (pure allosteric agonist) and compound 12 and SR146131 (PAM-agonists), as a result of Prime-mmGBSA calculations in the presence of CCK peptide. Within TM7, changes in Tyr 7.43 seem to have a downstream impact on Thr 7.44 and Ser 7.45 (not shown for clarity), suggesting a potential signal transduction mechanism through TM7. Further changes down TM7 were not observed, probably due to the 10 Å radius limit selected for the Prime-mmGBSA induced-fit calculation. The most striking differences were observed for TM2, probably driven by the combination of changes relative to Asn 2.61 and Asn 2.65, and to a lesser extent Pro 2.64. The top of TM2 was pushed the most in the complex with compound 10 and the least in the complex with SR146131. This shift in TM2 had impact on ECL1 position. In addition, Phe 198, which is present in ECL2, was also slightly shifted as well as the loop overall. ECL1 and ECL2 participate in CCK peptide binding and the predicted differences in ligand conformations would provide a different environment for the peptide, leading to potential changes in affinity, residence time and consequent functional effects.

Figure 13 summarizes the calculated relative binding affinities for each ligand with or without CCK peptide present in the binding site. In general, we see a decrease in relative binding affinities (ΔG) with or without CCK peptide, which is in correlation with decrease in potency as determined experimentally (see Table 3). We observe a more favorable (more negative) ΔG in the presence of CCK peptide for approximately half of the compounds, including SR146131 and compound 12, both with PAM-agonist properties. Compound 10 and compound 4, both experimentally shown to lack PAM activity, were the only two compounds with a more favorable ΔG in absence of CCK peptide. The other compounds did not display any large change in ΔG (Fig. 13). This provides qualitative insights into the complexes with various compounds, however, a more quantitative assessment of

Molecular Pharmacology Fast Forward. Published on December 27, 2018 as DOI: 10.1124/mol.118.114082
This article has not been copyedited and formatted. The final version may differ from this version.

binding affinities and functional effects would require more detailed calculations with large scale conformational sampling using molecular dynamics simulations and replica exchange methods.

Molecular Pharmacology Fast Forward. Published on December 27, 2018 as DOI: 10.1124/mol.118.114082
This article has not been copyedited and formatted. The final version may differ from this version.

Discussion

CCK induces satiety by acting on the CCK1R present on axonal projections of vagal afferent neurons present in the gut (Li and Owyang, 1994; Smith et al., 1981; Smith et al., 1985). This has provided a rationale for attempts to develop agonists of this receptor as non-caloric satiety agents, potentially useful for the management of obesity (Aquino et al., 1996; Berger et al., 2008; Elliott et al., 2010). Several synthetic agonists that have been developed for this purpose, however, none has gained regulatory approval for this application. This is mainly due to failure to reach the desired efficacy in humans (Jordan et al., 2008), with more potent analogs often possessing side effects, and longer duration agonists avoided due to concerns about potential trophic effects (Hoshi and Logsdon, 1993; Smith and Solomon, 2014).

We have proposed a possible alternative strategy to circumvent the concerns about side effects and possible toxicity of a highly potent full agonist, by working to develop CCK1R ligands with pure positive allosteric modulator activity for CCK, without possessing any intrinsic agonist activity (Desai et al., 2015a; Desai et al., 2016a; Desai et al., 2017; Desai et al., 2016b; Desai et al., 2015b; Miller and Desai, 2016). In this approach, the modulator would be expected to remain 'silent' in the absence of CCK, but then to act as a PAM to enhance the activity of CCK at the CCK1R only during the brief interval after meals when the hormone is released, thereby minimizing on-target side effects and possible toxicity. It also reduces the likelihood of desensitization. Indeed, this strategy has been successfully utilized at other receptors, including the G protein-coupled calcium-sensing receptor and the ionotropic GABA-A receptor (Barker et al., 1986; Nemeth et al., 2004). In addition to the usefulness of high throughput screening for such candidates, we have also postulated an alternate strategy where the determinants of agonist activity of an existing synthetic agonist can be removed, while retaining the components for causing a conformational change of the receptor to stabilize G protein association by reducing the energy barrier to achieve the active state (Desai et al., 2015b).

In the current study we demonstrate that SR146131, which is a CCK1R-specific, highly potent agonist (Bignon et al., 1999), also possesses PAM activity, hence categorizing it as a PAM-agonist. Thus, this compound is distinct from the previously characterized 1,5-benzodiazepine agonist, GI181771X (Desai et al., 2015b). Subsequent use of CCK1R-CCK2R TM chimeric constructs enabled development of a molecular model for compound binding to the CCK1R where SR146131 was accommodated in the same agonist pocket as that predicted for GI181771X. Of note, this modeling predicted different docking poses of SR146131 compared to previous models that were developed prior to our current understanding of class A GPCR crystal structures (Gouldson et al., 2000).

Since the receptor conformation elucidated in initial docking of SR146131 was not substantially different from that achieved using GI181771X, we hypothesized that the region critical for agonist activity could also be in analogous parts of both ligands. In the case of GI181771X, the isopropyl group interacts with Leu 7.39, which is a major determinant of the agonist activity (Harikumar et al., 2013). The portion of SR146131 that was predicted to be adjacent to this part of the receptor is the phenyl ring. Indeed, while that ring is present in the structurally-related antagonist, SR27897, it does not include the two methoxy groups present on the agonist. For this reason, these were a focus of interest in attempts to reduce agonist activity of the parent PAM-agonist.

We examined thirteen compounds that were structurally similar or related to SR146131 with substitutions on the phenyl ring and observed that the intrinsic agonist activity was reduced by varying degrees. We selected compounds 2, 4, and 12 from the series based on single point PAM assays testing the effect of different concentrations of compounds on the EC_{50} value of CCK. Further experiments with these compounds revealed that compound 12 exhibited the most notable positive cooperativity with CCK. This cooperativity was maintained in cells with both high and low levels of receptor expression, with the amount of intrinsic agonist activity reduced in the setting of low receptor expression, consistent with Monod-Wyman-Changeux mechanism model, as has been described for M1 muscarinic acetylcholine receptor PAMs (Canals et al., 2012).

Molecular Pharmacology Fast Forward. Published on December 27, 2018 as DOI: 10.1124/mol.118.114082
This article has not been copyedited and formatted. The final version may differ from this version.

Similar to SR146131, the degree of PAM activity of compound 12 was predicted to be greater when enhancing the action of the partial agonist, CCK-OPE. These data are illustrative of probe-dependency in allosterism that follows the Monod-Wyman-Changeux model, and is consistent with some M_1 muscarinic acetylcholine receptor PAMs (Canals et al., 2012). This enhancement of a weak response of a partial agonist has also been recorded for other receptors such as the $GABA_B$ receptor where the PAM exhibited an increase in E_{max} along with increase in potency of a partial agonist, as opposed to only a left-shift in EC_{50} for a full agonist (Maksay et al., 2000). Greater enhancement, relative to the GLP-1, of oxyntomodulin, or the GLP-1 metabolite GLP-1(9-36)NH2 that are weak or partial agonists, has also been observed with small molecule PAMs at the GLP1-R (Koole et al.; Wootten et al., 2012). It is important to note that CCK-OPE is not a natural metabolite of CCK, and therefore, these data do not hold physiologic importance, however it is an important tool to understand the compound pharmacology. Based on these observations, it might be interesting to explore whether a combination therapy with a partial agonist and this type of PAM would have therapeutic advantages over use of only the PAM itself.

It is important to note that in the case of SR146131 and the structurally-related compounds tested in this study, the observed potency tracked with the affinity of the compounds resulting in PAM-agonists with varying degrees of activity. For these compounds, the PAM activity is dependent on their ability to stabilize an “active” conformation of the receptor that provides a lower energy barrier threshold for activation by the co-bound orthosteric peptide; this is linked to their intrinsic agonist activity. Prime-mmGBSA calculations on the complexes of small molecules bound to the receptor-peptide system show differences in ΔG for these analogs, which is in qualitative agreement with their observed agonist or PAM-agonist functional effects. However, as this series of compounds appear to follow the Monod-Wyman-Changeaux model of allosterism (Canals et al., 2012), it may be difficult to dissect the agonist activity from the PAM activity to achieve a pure PAM without intrinsic agonist activity. This phenomenon is also an issue for certain scaffolds of M1 muscarinic acetylcholine receptor PAM-agonists (Miao et al., 2016), but can be overcome with alternative scaffolds (Khajehali et al., 2018).

Cinacalcet, a PAM of the calcium-sensing receptor, has rather small PAM activity for calcium at this receptor and had nonetheless been approved by the FDA in 2004. However, in this particular case, where the serum concentrations of the endogenous ligand are tightly regulated, only a small change in the activity of the agonist is necessary, and even in some cases better than a large effect that could stimulate side-effects. Of note, the small shift in potency by Cinacalcet is complemented by a higher cooperativity of the compound (Davey et al., 2012). However, such level of detail on fine-tuning the CCK1R function physiologically does not yet exist. Therefore, further experimentation is required to understand the desired magnitude of PAM activity at the CCK1R and will likely require identification of a novel scaffold with no intrinsic efficacy.

In conclusion, we report that SR146131 is a PAM-agonist that binds to an allosteric pocket of the CCK1R (Harikumar et al., 2013). Based on the proposed binding pose for SR146131 within this pocket, we postulate that the methoxy groups are important for the agonist activity. By studying analogs of SR146131 with different phenyl substitutions both *in vitro* and *in silico*, we gained further insights into the mode of small molecule ligand binding and receptor activation, and the interactions between CCK1R, PAMs and CCK that drive agonism and cooperative behavior. These insights are important for future drug design towards a PAM without intrinsic agonist activity that might be useful for the therapy of obesity.

Acknowledgements

The authors would like to thank Sanofi for providing analogs of SR146131, Dr. David Thorpe for initiating this collaboration, and Dr. Maoqing Dong for help in manuscript preparation.

Authorship Contributions

Participated in research design: Desai, Mechin, Sexton, Christopoulos, Miller

Conducted experiments: Desai, Mechin, Nagarajan, Lam, Nair

Performed data analysis: Desai, Mechin, Nagarajan, Valant, Wootten, Nair, Sexton, Christopoulos, Miller

Wrote or contributed to the writing of the manuscript: Desai, Mechin, Nagarajan, Valant, Wootten, Lam, Orry, Abagyan, Nair, Sexton, Christopoulos, Miller

References

Akgun E, Korner M, Gao F, Harikumar KG, Waser B, Reubi JC, Portoghese PS and Miller LJ (2009) Synthesis and in vitro characterization of radioiodinatable benzodiazepines selective for type 1 and type 2 cholecystokinin receptors. *J Med Chem* **52**:2138-2147.

Aquino CJ, Armour DR, Berman JM, Birkemo LS, Carr RA, Croom DK, Dezube M, Dougherty RW, Jr., Ervin GN, Grizzle MK, Head JE, Hirst GC, James MK, Johnson MF, Miller LJ, Queen KL, Rimele TJ, Smith DN and Sugg EE (1996) Discovery of 1,5-benzodiazepines with peripheral cholecystokinin (CCK-A) receptor agonist activity. 1. Optimization of the agonist "trigger". *J Med Chem* **39**:562-569.

Ballesteros JA and Weinstein H (1992) Analysis and refinement of criteria for predicting the structure and relative orientations of transmembranal helical domains. *Biophys J* **62**:107-109.

Barker JL, Harrison NL and Mariani AP (1986) Benzodiazepine pharmacology of cultured mammalian CNS neurons. *Life Sci* **39**:1959-1968.

Berger R, Zhu C, Hansen AR, Harper B, Chen Z, Holt TG, Hubert J, Lee SJ, Pan J, Qian S, Reitman ML, Strack AM, Weingarth DT, Wolff M, Macneil DJ, Weber AE and Edmondson SD (2008) 2-Substituted piperazine-derived imidazole carboxamides as potent and selective CCK1R agonists for the treatment of obesity. *Bioorg Med Chem Lett* **18**:4833-4837.

Bignon E, Alonso R, Arnone M, Boigegrain R, Brodin R, Gueudet C, Heaulme M, Keane P, Landi M, Molimard JC, Olliero D, Poncelet M, Seban E, Simiand J, Soubrie P, Pascal M, Maffrand JP and Le Fur G (1999) SR146131: a new potent, orally active, and selective nonpeptide cholecystokinin subtype 1 receptor agonist. II. In vivo pharmacological characterization. *J Pharmacol Exp Ther* **289**:752-761.

Bowers KJ, Chow E, Xu H, Dror RO, Eastwood MP, Gregersen BA, Klepeis JL, Kolossváry I, Moraes MA, Sacerdoti FD, Salmon JK, Shan Y and Shaw DE (2006) Scalable algorithms for molecular dynamics simulations on commodity clusters. *Proc ACM/IEEE Conf Supercomputing*:Tampa, Florida, Nov 11–17, 2006.

Canals M, Lane JR, Wen A, Scammells PJ, Sexton PM and Christopoulos A (2012) A Monod-Wyman-Changeux mechanism can explain G protein-coupled receptor (GPCR) allosteric modulation. *J Biol Chem* **287**:650-659.

Cawston EE, Lam PC, Harikumar KG, Dong M, Ball AM, Augustine ML, Akgun E, Portoghese PS, Orry A, Abagyan R, Sexton PM and Miller LJ (2012) Molecular basis for binding and subtype selectivity of 1,4-benzodiazepine antagonist ligands of the cholecystokinin receptor. *J Biol Chem* **287**:18618-18635.

Chaudhri OB, Salem V, Murphy KG and Bloom SR (2008) Gastrointestinal satiety signals. *Annu Rev Physiol* **70**:239-255.

Cheng Y and Prusoff WH (1973) Relationship between the inhibition constant (K1) and the concentration of inhibitor which causes 50 per cent inhibition (I50) of an enzymatic reaction. *Biochem Pharmacol* **22**:3099-3108.

Christopoulos A and Kenakin T (2002) G protein-coupled receptor allosterism and complexing. *Pharmacol Rev* **54**:323-374.

Davey AE, Leach K, Valant C, Conigrave AD, Sexton PM and Christopoulos A (2012) Positive and negative allosteric modulators promote biased signaling at the calcium-sensing receptor. *Endocrinology* **153**:1232-1241.

Desai AJ, Dong M, Harikumar KG and Miller LJ (2015a) Impact of ursodeoxycholic acid on a CCK1R cholesterol-binding site may contribute to its positive effects in digestive function. *Am J Physiol* **309**:G377-386.

Desai AJ, Dong M, Harikumar KG and Miller LJ (2016a) Cholecystokinin-induced satiety, a key gut servomechanism that is affected by the membrane microenvironment of this receptor. *Int J Obes Supp* **6**:S22-S27.

Desai AJ, Dong M, Langlais BT, Dueck AC and Miller LJ (2017) Cholecystokinin responsiveness varies across the population dependent on metabolic phenotype. *Am J Clin Nutr* **106**:447-456.

Desai AJ, Dong M and Miller LJ (2016b) Beneficial effects of beta-sitosterol on type 1 cholecystokinin receptor dysfunction induced by elevated membrane cholesterol. *Clin Nutr* **35**:1374-1379.

Desai AJ, Harikumar KG and Miller LJ (2014) A type 1 cholecystokinin receptor mutant that mimics the dysfunction observed for wild type receptor in a high cholesterol environment. *J Biol Chem* **289**:18314-18326.

Desai AJ, Henke BR and Miller LJ (2015b) Elimination of a cholecystokinin receptor agonist 'trigger' in an effort to develop positive allosteric modulators without intrinsic agonist activity. *Bioorg Med Chem Lett* **25**:1849-1855.

Desai AJ, Lam PC, Orry A, Abagyan R, Christopoulos A, Sexton PM and Miller LJ (2015c) Molecular Mechanism of Action of Triazolobenzodiazepinone Agonists of the Type 1 Cholecystokinin Receptor. Possible Cooperativity across the Receptor Homodimeric Complex. *J Med Chem* **58**:9562-9577.

Ding XQ, Dolu V, Hadac EM, Holicky EL, Pinon DI, Lybrand TP and Miller LJ (2001) Refinement of the structure of the ligand-occupied cholecystokinin receptor using a photolabile amino-terminal probe. *J Biol Chem* **276**:4236-4244.

Ding XQ, Pinon DI, Furse KE, Lybrand TP and Miller LJ (2002) Refinement of the conformation of a critical region of charge-charge interaction between cholecystokinin and its receptor. *Mol Pharmacol* **61**:1041-1052.

Dong M, Lam PC, Pinon DI, Abagyan R and Miller LJ (2009) Elucidation of the molecular basis of cholecystokinin Peptide docking to its receptor using site-specific intrinsic photoaffinity labeling and molecular modeling. *Biochemistry* **48**:5303-5312.

Ehlert FJ (1988) Estimation of the affinities of allosteric ligands using radioligand binding and pharmacological null methods. *Mol Pharmacol* **33**:187-194.

Elliott RL, Cameron KO, Chin JE, Bartlett JA, Beretta EE, Chen Y, Jardine Pda S, Dubins JS, Gillaspy ML, Hargrove DM, Kalgutkar AS, LaFlamme JA, Lame ME, Martin KA, Maurer TS, Nardone NA, Oliver RM, Scott DO, Sun D, Swick AG, Trebino CE and Zhang Y (2010) Discovery of N-benzyl-2-[(4S)-4-(1H-indol-3-ylmethyl)-5-oxo-1-phenyl-4,5-dihydro-6H-[1,2,4]tri azolo[4,3-a][1,5]benzodiazepin-6-yl]-N-isopropylacetamide, an orally active, gut-selective CCK1 receptor agonist for the potential treatment of obesity. *Bioorg Med Chem Lett* **20**:6797-6801.

Escrieut C, Gigoux V, Archer E, Verrier S, Maigret B, Behrendt R, Moroder L, Bignon E, Silvente-Poirot S, Pradayrol L, Fourmy D. (2002) The biologically crucial C terminus of cholecystokinin and the non-peptide agonist SR-146,131 share a common binding site in the human CCK1 receptor. Evidence for a crucial role of Met-121 in the activation process. *J Biol Chem* **277**:7546-7555.

Friesner RA, Banks JL, Murphy RB, Halgren TA, Klicic JJ, Mainz DT, Repasky MP, Knoll EH, Shelley M, Perry JK, Shaw DE, Francis P and Shenkin PS (2004) Glide: a new approach for rapid, accurate docking and scoring. 1. Method and assessment of docking accuracy. *J Med Chem* **47**:1739-1749.

Gaisano HY, Klueppelberg UG, Pinon DI, Pfenning MA, Powers SP and Miller LJ (1989) Novel tool for the study of cholecystokinin-stimulated pancreatic enzyme secretion. *J Clin Invest* **83**:321-325.

Gibbs J, Young RC and Smith GP (1973) Cholecystokinin decreases food intake in rats. *J Comp Physiol Psychol* **84**:488-495.

Gigoux V, Escrieut C, Silvente-Poirot S, Maigret B, Gouilleux L, Fehrentz JA, Gully D, Moroder L, Vaysse N and Fourmy D (1998) Met-195 of the cholecystokinin-A receptor interacts with the sulfated tyrosine of cholecystokinin and is crucial for receptor transition to high affinity state. *J Biol Chem* **273**:14380-14386.

Gigoux V, Maigret B, Escrieut C, Silvente-Poirot S, Bouisson M, Fehrentz JA, Moroder L, Gully D, Martinez J, Vaysse N and Fourmy AD (1999) Arginine 197 of the cholecystokinin-A receptor binding site interacts with the sulfate of the peptide agonist cholecystokinin. *Protein Sci* **8**:2347-2354.

Giragossian C and Mierke DF (2001) Intermolecular interactions between cholecystokinin-8 and the third extracellular loop of the cholecystokinin A receptor. *Biochemistry* **40**:3804-3809.

Gouldson P, Legoux P, Carillon C, Delpech B, Le Fur G, Ferrara P and Shire D (2000) The agonist SR 146131 and the antagonist SR 27897 occupy different sites on the human CCK(1) receptor. *Eur J Pharmacol* **400**:185-194.

Hadac EM, Dawson ES, Darrow JW, Sugg EE, Lybrand TP and Miller LJ (2006) Novel benzodiazepine photoaffinity probe stereoselectively labels a site deep within the membrane-spanning domain of the cholecystokinin receptor. *J Med Chem* **49**:850-863.

Hadac EM, Ghanekar DV, Holicky EL, Pinon DI, Dougherty RW and Miller LJ (1996) Relationship between native and recombinant cholecystokinin receptors: role of differential glycosylation. *Pancreas* **13**:130-139.

Hadac EM, Pinon DI, Ji Z, Holicky EL, Henne RM, Lybrand TP and Miller LJ (1998) Direct identification of a second distinct site of contact between cholecystokinin and its receptor. *J Biol Chem* **273**:12988-12993.

Harikumar KG, Cawston EE, Lam PC, Patil A, Orry A, Henke BR, Abagyan R, Christopoulos A, Sexton PM and Miller LJ (2013) Molecular basis for benzodiazepine agonist action at the type 1 cholecystokinin receptor. *J Biol Chem* **288**:21082-21095.

Hoshi H and Logsdon CD (1993) Both low- and high-affinity CCK receptor states mediate trophic effects on rat pancreatic acinar cells. *Am J Physiol* **265**:G1177-1181.

Jacobson MP, Pincus DL, Rapp CS, Day TJ, Honig B, Shaw DE and Friesner RA (2004) A hierarchical approach to all-atom protein loop prediction. *Proteins* **55**:351-367.

Ji Z, Hadac EM, Henne RM, Patel SA, Lybrand TP and Miller LJ (1997) Direct identification of a distinct site of interaction between the carboxyl-terminal residue of cholecystokinin and the type A cholecystokinin receptor using photoaffinity labeling. *J Biol Chem* **272**:24393-24401.

Jordan J, Greenway FL, Leiter LA, Li Z, Jacobson P, Murphy K, Hill J, Kler L and Aftring RP (2008) Stimulation of cholecystokinin-A receptors with GI181771X does not cause weight loss in overweight or obese patients. *Clin Pharmacol Ther* **83**:281-287.

Kennedy K, Gigoux V, Escrieut C, Maigret B, Martinez J, Moroder L, Frehel D, Gully D, Vaysse N and Fourmy D (1997) Identification of two amino acids of the human cholecystokinin-A receptor that interact with the N-terminal moiety of cholecystokinin. *J Biol Chem* **272**:2920-2926.

Khajehali E, Valant C, Jorg M, Tobin AB, Conn PJ, Lindsley CW, Sexton PM, Scammells PJ and Christopoulos A (2018) Probing the binding site of novel selective positive allosteric modulators at the M1 muscarinic acetylcholine receptor. *Biochem Pharmacol* **154**:243-254.

Kissileff HR, Pi-Sunyer FX, Thornton J and Smith GP (1981) C-terminal octapeptide of cholecystokinin decreases food intake in man. *Am J Clin Nutr* **34**:154-160.

Koole C, Wootten D, Simms J, Valant C, Sridhar R, Woodman OL, Miller LJ, Summers RJ, Christopoulos A and Sexton PM Allosteric ligands of the glucagon-like peptide 1 receptor (GLP-1R) differentially modulate endogenous and exogenous peptide responses in a pathway-selective manner: implications for drug screening. *Mol Pharmacol* **78**:456-465.

Labute P (2010) LowModeMD--implicit low-mode velocity filtering applied to conformational search of macrocycles and protein loops. *J Chem Inf Model* **50**:792-800.

Latorraca NR, Venkatakrishnan AJ and Dror RO (2017) GPCR Dynamics: Structures in Motion. *Chem Rev* **117**:139-155.

Leach K, Sexton PM and Christopoulos A (2007) Allosteric GPCR modulators: taking advantage of permissive receptor pharmacology. *Trends Pharmacol Sci* **28**:382-389.

Li Y and Owyang C (1994) Endogenous cholecystokinin stimulates pancreatic enzyme secretion via vagal afferent pathway in rats. *Gastroenterology* **107**:525-531.

Maksay G, Thompson SA and Wafford KA (2000) Allosteric modulators affect the efficacy of partial agonists for recombinant GABA(A) receptors. *Br J Pharmacol* **129**:1794-1800.

May LT, Avlani VA, Langmead CJ, Herdon HJ, Wood MD, Sexton PM and Christopoulos A (2007) Structure-function studies of allosteric agonism at M2 muscarinic acetylcholine receptors. *Mol Pharmacol* **72**:463-476.

Miao Y, Goldfeld DA, Moo EV, Sexton PM, Christopoulos A, McCammon JA and Valant C (2016) Accelerated structure-based design of chemically diverse allosteric modulators of a muscarinic G protein-coupled receptor. *Proc Natl Acad Sci USA* **113**:E5675-5684.

Miller LJ and Desai AJ (2016) Metabolic Actions of the Type 1 Cholecystokinin Receptor: Its Potential as a Therapeutic Target. *Trends Endocrinol Metab* **27**:609-619.

Nemeth EF, Heaton WH, Miller M, Fox J, Balandrin MF, Van Wagenen BC, Colloton M, Karbon W, Scherrer J, Shatzen E, Rishton G, Scully S, Qi M, Harris R, Lacey D and Martin D (2004) Pharmacodynamics of the type II calcimimetic compound cinacalcet HCl. *J Pharmacol Exp Ther* **308**:627-635.

Pellegrini M and Mierke DF (1999) Molecular complex of cholecystokinin-8 and N-terminus of the cholecystokinin A receptor by NMR spectroscopy. *Biochemistry* **38**:14775-14783.

Powers SP, Pinon DI and Miller LJ (1988) Use of N,O-bis-Fmoc-D-Tyr-ONSu for introduction of an oxidative iodination site into cholecystokinin family peptides. *Int J Pept Protein Res* **31**:429-434.

Rasmussen SG, DeVree BT, Zou Y, Kruse AC, Chung KY, Kobilka TS, Thian FS, Chae PS, Pardon E, Calinski D, Mathiesen JM, Shah ST, Lyons JA, Caffrey M, Gellman SH, Steyaert J, Skiniotis G, Weis WI, Sunahara RK and Kobilka BK (2011) Crystal structure of the beta2 adrenergic receptor-Gs protein complex. *Nature* **477**:549-555.

Sherman W, Day T, Jacobson MP, Friesner RA and Farid R (2006) Novel procedure for modeling ligand/receptor induced fit effects. *J Med Chem* **49**:534-553.

Smith GP, Jerome C, Cushin BJ, Eterno R and Simansky KJ (1981) Abdominal vagotomy blocks the satiety effect of cholecystokinin in the rat. *Science* **213**:1036-1037.

Smith GP, Jerome C and Norgren R (1985) Afferent axons in abdominal vagus mediate satiety effect of cholecystokinin in rats. *Am J Physiol* **249**:R638-641.

Smith JP and Solomon TE (2014) Cholecystokinin and pancreatic cancer: the chicken or the egg? *Am J Physiol* **306**:G91-G101.

Totrov M (2008) Atomic property fields: generalized 3D pharmacophoric potential for automated ligand superposition, pharmacophore elucidation and 3D QSAR. *Chem Biol Drug Des* **71**:15-27.

Totrov M and Abagyan R (1997) Flexible protein-ligand docking by global energy optimization in internal coordinates. *Proteins* **Suppl 1**:215-220.

Watts KS, Dalal P, Tebben AJ, Cheney DL and Shelley JC (2014) Macrocycle conformational sampling with MacroModel. *J Chem Inf Model* **54**:2680-2696.

Wootten D, Savage EE, Valant C, May LT, Sloop KW, Ficorilli J, Showalter AD, Willard FS, Christopoulos A and Sexton PM (2012) Allosteric modulation of endogenous metabolites as an avenue for drug discovery. *Mol Pharmacol* **82**:281-290.

Yin J, Babaoglu K, Brautigam CA, Clark L, Shao Z, Scheuermann TH, Harrell CM, Gotter AL, Roecker AJ, Winrow CJ, Renger JJ, Coleman PJ and Rosenbaum DM (2016) Structure and ligand-binding mechanism of the human OX1 and OX2 orexin receptors. *Nat Struct Mol Biol* **23**:293-299.

Molecular Pharmacology Fast Forward. Published on December 27, 2018 as DOI: 10.1124/mol.118.114082
This article has not been copyedited and formatted. The final version may differ from this version.

Footnotes

This work was partially supported by the Mayo Clinic and by a grant from the Flinn Foundation. D.W., P.M.S. and A.C. are Career Development, Principal, and Senior Principal Research Fellows, respectively, of the National Health and Medical Research Council of Australia.

Address correspondence to: Laurence J. Miller, M.D., Mayo Clinic, 13400 East Shea Blvd, Scottsdale, AZ 85259. E-mail: miller@mayo.edu

Molecular Pharmacology Fast Forward. Published on December 27, 2018 as DOI: 10.1124/mol.118.114082
This article has not been copyedited and formatted. The final version may differ from this version.

Figure Legends

Fig. 1. Properties of SR146131. Shown is the structure of SR146131 (A), along with intracellular calcium responses generated at both subtypes of CCK receptors stably expressed on CHO cells (B). Data are represented as means ± S.E.M. of eight experiments. Shown also are the data from competition-binding studies with the allosteric antagonist radioligands, ^{125}I-BDZ-1 at the CCK1R or ^{125}I-BDZ-2 at the CCK2R stably expressed on CHO cell membranes (C). Non-saturable binding was determined by using 1 μM unlabeled BDZ. Data are represented as means ± S.E.M. of data from six experiments for CCK1R and five experiments for CCK2R.

Fig. 2. Effect of increasing concentrations of SR146131 on CCK- and CCK-OPE-stimulated intracellular calcium responses. Shown are CCK-stimulated intracellular calcium dose-response curves on CHO-CCK1R cells in the absence or presence of increasing concentrations of SR146131. Data represent means ± S.E.M. of data from six (0), four ($1e^{-12}$), seven ($1e^{-11}$), and nine ($3.16e^{-11}$) experiments (A). Shown also are the data generated from similar experiments performed using the partial agonist, CCK-OPE, on the same cells (B). Values are expressed as percentages of the intracellular calcium responses to maximum stimulation achieved by 0.1 mM ATP. Data represent means ± S.E.M. of data from seven (0), eight ($1e^{-13}$), and four ($3.16e^{-13}$), six ($1e^{-12}$), and seven ($3.16e^{-12}$) experiments.

Fig. 3. Biological activity and competition-binding studies of SR146131 at CCK1R- and CCK2R-based chimeric receptor constructs. The dose-response curves shown here represent the ability of SR146131 to stimulate intracellular calcium responses in CHO cells bearing CCK1R (A) or CCK2R (B) wild type and chimeric constructs. Data are represented in percentage responses relative to the maximum stimulation achieved by 0.1 mM ATP. Shown also are the competition-binding curves for SR146131 at CCK1R-based (C) or CCK2R-based (D) TM chimeric constructs using the allosteric antagonist radioligands, ^{125}I-BDZ-1 (for CCK1R) and ^{125}I-BDZ-2 (for CCK2R). Values represent percentages of maximal saturable binding that were observed in the absence of competitor. Non-

saturable binding was determined by using 1 μM unlabeled BDZ-1 or BDZ-2, as appropriate for the radioligand. Data are expressed as means ± S.E.M. of data from six experiments.

Fig. 4. Docking of SR146131 at the CCK1R. Shown is the best performing model for docked binding poses of SR146131 (green stick) to CCK1R (grey ribbon and stick) (A, B). The viewpoint in (A) is from the side within the membrane with TM1 cut away, and that in (B) is from above the membrane. Part of TM7 has been cut away for optimal viewing of the interactions. This model in PDB format is provided in Supplementary Data file, S1.

Fig. 5. Comparison between docking of SR146131 and GI181771X at the CCK1R. The key predicted interactions between SR146131 (green stick) and CCK1R that were studied by mutation are shown in light grey stick and ribbon in (A). Residues Trp 6.48 (W326A), Met 3.32 (M121A), and Val 3.36 (V125A) make contact area interaction of 17 $Å^2$, 40 $Å^2$, and 21 $Å^2$, with SR146131. Ser 7.42 (S359A) and Asn 2.65 (N102A) do not make contacts with SR146131, but make hydrogen bond interactions with other side-chains (purple spheres) which are predicted to stabilize the conformation of the pocket. Ser 7.42 makes two hydrogen bonds with the backbone atoms of TM7 and Asn 2.65 is one part of a chain of hydrogen bonds with Asn 2.61 and Tyr 7.43. Panel (B) shows a comparison of the docked binding pose of SR146131 (green stick) and GI181771X (purple stick): part of TM7 has been cut away for optimal viewing of the interactions. The pose of GI181771X is consistent with that reported in Harikumar et al., 2013 and docks in a similar region of the pocket as SR146131, with the thiazole ring of SR146131 and the benzodiazepine ring of GI181771X occupying the same space. The main differences are that GI181771X makes closer interactions with TM6 including two hydrogen bonds (small colored spheres) with Asn 6.55 and Arg 6.58. Inset: a close-up of the isopropyl group important for agonist activity of GI181771X. In SR146131, the carbon atom of the 5-methoxy group overlays this region of GI181771X. This model in PDB format is provided in Supplementary Data files, S1 (SR146131) and S2 (GI181771X).

Fig. 6. Impact of selected receptor mutations on SR146131 biological activity and binding. Shown are the effects of alanine replacements of the residues predicted by the molecular model as potentially

interacting with SR146131, on the biological activity (A) and binding (B) of the compound. Data are expressed as means ± S.E.M. of data from eleven (WT), seven (M121A), six (V125A), seven (W326A), and seven (S359A) experiments (A), and ten (WT), six (M121A, V125A, W326A), and eight (S359A) experiments (B).

Fig. 7. Structures of compounds 2, 4, and 12. Shown is the region of SR146141 that is analogous to the isopropyl group of GI181771X, which has been shown to be critical for its agonist activity, shaded in gray (A), along with structures of compound 2 (B), 4 (C), and 12 (D).

Fig. 8. Effect of increasing concentrations of compounds 2 and 4 on CCK-stimulated intracellular calcium responses. Shown are CCK-stimulated intracellular calcium dose-response curves on CHO-CCK1R cells in the absence or presence of increasing concentrations of compound 2 (A), and compound 4 (B), with values expressed as percentages of the response to maximum stimulation achieved by 0.1 mM ATP. Data represent means ± S.E.M. of data from five ($10e^{-9}$, $5e^{-9}$, $2.5e^{-9}$, $1e^{-9}$), three ($0.1e^{-9}$), and six (0) experiments (A), and nine experiments for all doses (B).

Fig. 9. Effect of increasing concentrations of compound 12 on CCK- and CCK-OPE-stimulated calcium responses. Shown are effects of increasing concentrations of compound 12 on CCK-stimulated intracellular calcium dose-response curves in CHO cells stably expressing CCK1R at 19.2 ± 2.5 pmol/mg (A). Shown also are the data generated from analogous experiments performed using the partial agonist, CCK-OPE (B). Values are expressed as percentages of the response to maximum stimulation achieved by 0.1 mM ATP. Data represent means ± S.E.M. of data from eleven (0, $0.5e^{-9}$, $1e^{-9}$), nine ($0.25e^{-9}$), and twelve ($0.05e^{-9}$, $0.1e^{-9}$) experiments (A), and six ($3.16e^{-11}$), nine ($1e^{-12}$, $3.16e^{-12}$, $1e^{-11}$, $1e^{-10}$), seven ($1e^{-13}$, $3.16e^{-13}$) and fourteen (0) experiments (B).

Fig. 10. Model of CCK and compound 12 bound to the CCK1R. Shown is a representation of the ternary structures of the CCK1R (in light grey) docked with the CCK peptide (in green) and the positive allosteric modulator compound 12 (in cyan) for binding mode 1 (A), where the acid group is involved in a salt bridge with Arg 6.58, and for binding mode 2 (B), where the acid group is involved in a H-bond with Asn 6.55 side chain. In both cases, potential H-bonds are represented with light blue

dashed lines. Some helices and residues were clipped for clarity. These models in PDB format are provided in Supplementary Data files, S3 (mode 1) and S4 (mode 2).

Fig. 11. Comparison between the docking of compound 12 and SR146131 at CCK1R. A comparison of receptor interacting residues in the docked binding poses of SR146131 (purple stick) and compound 12 (cyan stick) is shown for binding mode 1 (A), and 2 (B). CCK is shown in light green. The differences between both compounds in substitutions on the benzene ring postulated to be important for its agonist activity, led to differences in interaction with Leu 7.39 and Ser 7.42, as well as Asn 2.65. Some helices and residues were clipped for clarity. These models in PDB format are provided in Supplementary Data files S3 (mode 1, compound 12), S4 (mode 2, compound 12), S5 (mode 1, SR146131) and S6 (mode 2, SR146131).

Fig. 12. Comparison between the Prime-mmGBSA calculations for SR146131 (ago-PAM), compound 10 (allosteric agonist) and compound 12 (PAM). CCK1R-SR146131 complex is shown in blue, CCK1R-compound 10 complex shown in green and CCK1R-compound 12 complex shown in magenta. Differences in side chain orientations in the vicinity of the substituted benzene ring are shown, while all other CCK1R residues are hidden for clarity. The CCK peptide is represented by an orange ribbon in all three cases.

Fig. 13. Prime-mmGBSA values for all compounds in the presence or absence of CCK. Compounds in this graph are illustrated in the order of decreasing potency of agonist activity. Blue bars correspond to Prime-mmGBSA calculations in the presence of CCK peptide, while red bars correspond to the same calculations after removal of the CCK peptide. Prime-mmGBSA relative binding energies (in Kcal/mol) are noted below each bar.

Molecular Pharmacology Fast Forward. Published on December 27, 2018 as DOI: 10.1124/mol.118.114082
This article has not been copyedited and formatted. The final version may differ from this version.

TABLE 1

Pharmacology of SR146131 at WT and chimeric CCK1R and CCK2R

[1]Equilibrium binding was established using the CCK1R-selective small molecule radioligand, ^{125}I-BDZ-1.

[2]Equilibrium binding was established using the CCK2R-selective small molecule radioligand, ^{125}I-BDZ-2.

Data are mean ± S.E.M. from a minimum of 4 independent experiments conducted in duplicate. pKb and Log α were derived from fitting to an allosteric model of binding (Eq. 1). Differences in receptor binding and signalling parameters between constructs were evaluated using one way ANOVA with Dunnett's post-test. * $p<0.05$, $^{**}p<0.01$, relative values compared with wild type receptor. NDB: No detectable binding, NR: No response.

CCK1R-based chimeric receptors[1]	**Receptor abbreviations**	**pIC_{50}**	**pEC_{50}**	**pK_b**	**Log α**
CCK1R WT	CCK1R	8.10 ± 0.09	10.59 ± 0.11	8.20 ± 0.08	-1.20 ± 0.10
N2.61T	CCK1R TM2	6.85 ± 0.04**	9.70 ± 0.11**	7.30 ± 0.11**	-0.50 ± 0.04**
T3.28V, T3.29S	CCK1R TM3	9.13 ± 0.07**	10.13 ± 0.09*	9.14 ± 0.08**	(α is close to 0)**
I6.51V, F6.52Y	CCK1R TM6	7.26 ± 0.04**	10.12 ± 0.06*	7.60 ± 01**	-0.64 ± 0.08**
L7.39H	CCK1R TM7	6.33 ± 0.20**	8.00 ± 0.10**	7.24 ± 0.11**	-0.40 ± 0.05**
CCK2R-based chimeric receptors[2]					
CCK2R WT	CCK2R	6.23 ± 0.13	NR	7.20 ± 0.17	-0.36 ± 0.07
T2.61N	CCK2R TM2	NDB	NR	NDB	NDB
V3.28T, S3.29T	CCK2R TM3	5.94 ± 0.09	NR	7.06 ± 0.28	-0.24 ± 0.08
V6.51I, Y6.52F	CCK2R TM6	7.03 ± 0.13**	< 6.0	7.40 ± 0.12	-0.61 ± 0.05*
H7.39L	CCK2R TM7	8.03 ± 0.09**	< 6.0	8.11 ± 0.08**	-1.11 ± 0.06**

Molecular Pharmacology Fast Forward. Published on December 27, 2018 as DOI: 10.1124/mol.118.114082
This article has not been copyedited and formatted. The final version may differ from this version.

TABLE 2

SR146131 binding parameters and potency for CCK1R-based single mutant constructs

[1]intrinsic efficacy of SR146131 in each of the cell lines, compared with that in WT CCK1R. *p<0.05,** p<0.01, **** p<0.0001 relative values compared with wild type CCK1 receptor using one-way ANOVA, Dunnett's post-test.

CCK1R-based chimeric receptors	**Receptor abbreviations**	**pIC_{50}**	**pEC_{50}**	**Log τ_B corrected for Bmax[1]**
CCK1R WT	CCK1R	8.08 ± 0.10 (n=10)	10.34 ± 0.11 (n=8)	0.76 ± 0.09
M3.32A	CCK1R M121A	9.61 ± 0.15** (n=5)	9.90 ± 0.16* (n=4)	-1.62 ± 0.06****
V3.36A	CCK1R V125A	7.97 ± 0.13 (n=6)	9.60 ± 0.05** (n=5)	1.83 ± 0.11****
W6.48A	CCK1R W326A	8.14 ± 0.08 (n=6)	9.30 ± 0.06** (n=4)	1.44 ± 0.04****
S7.42A	CCK1R S359A	8.43 ± 0.07 (n=8)	10.92 ± 0.10** (n=5)	0.52 ± 0.09

Molecular Pharmacology Fast Forward. Published on December 27, 2018 as DOI: 10.1124/mol.118.114082
This article has not been copyedited and formatted. The final version may differ from this version.

TABLE 3

Substitutions at 'R' in the compounds structurally-related to SR146131. The series is arranged in descending order of potency

pEC_{50} values represent means ± SEM, * $p<0.05$, $^{**}p<0.01$, $^{***}p<0.001$ calculated using one-way ANOVA, Dunnett's post-test.

Positions	**2**	**3**	**4**	**5**	**6**	**Indole Substitutions**	**pEC_{50}**	**Emax**
SR 146131	**Methoxy**		**Cl**	**Methoxy**		**5,7-dimethyl**	**10.50±0.20**	
10	Methoxy		Me		Methoxy		10.17±0.17 (n=5)	124.4±7.7
12	Methoxy		Methoxy	Ethyl		5-methyl	8.81±0.12* (n=5)	103.7±4.6
9	Methoxy		Me	MethoxyMe			8.77±0.16* (n=5)	104.5±5.7
7	Me		Me	Methoxy			8.60±0.13* (n=5)	97.9±1.1
3	Methoxy		Cl	Cl			8.30±0.10* (n=5)	113.2±6.0
11	Methoxy		Methoxy	Me		5,7-dimethyl	8.30±0.10* (n=5)	102.9±4.4
4	Methoxy		Methoxy				8.22±0.14* (n=5)	92.5±5.4
2	Methoxy		Me	Me			8.17±0.14* (n=4)	94.7±6.4
8	Methoxy		dioxalane				7.72±0.18* (n=5)	73.7±9.4
1	Methoxy		Me	Cl			7.58±0.13* (n=4)	92.0±10.0
13	Cl						7.28±0.16* (n=5)	61.6±8.5**
5	Methoxy	Methoxy	Me				7.02±0.23* (n=3)	25.6±4.5***
6	Me	Me	Methoxy				6.85±0.18* (n=3)	19.0±8.5***

Molecular Pharmacology Fast Forward. Published on December 27, 2018 as DOI: 10.1124/mol.118.114082
This article has not been copyedited and formatted. The final version may differ from this version.

Figure 1

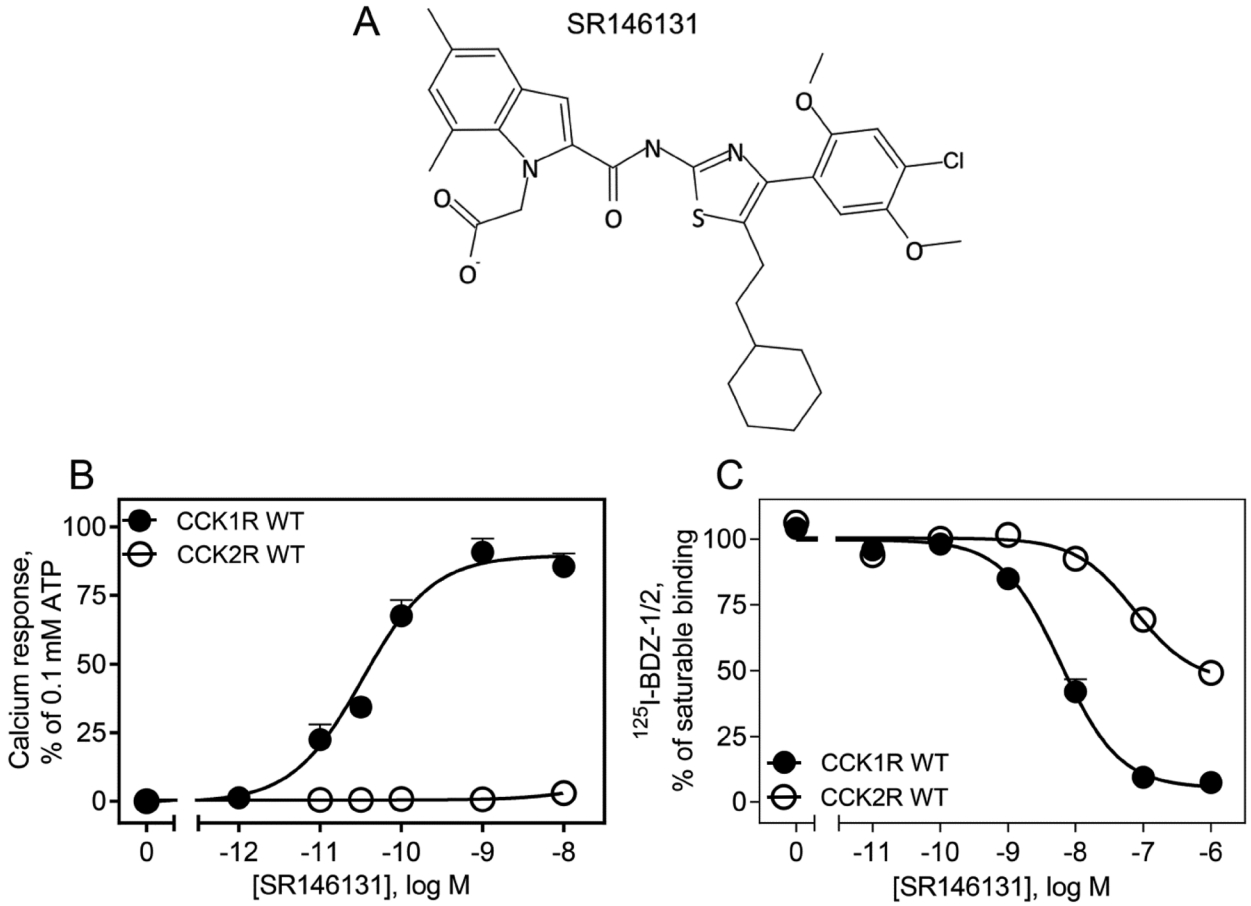

Molecular Pharmacology Fast Forward. Published on December 27, 2018 as DOI: 10.1124/mol.118.114082
This article has not been copyedited and formatted. The final version may differ from this version.

Figure 2

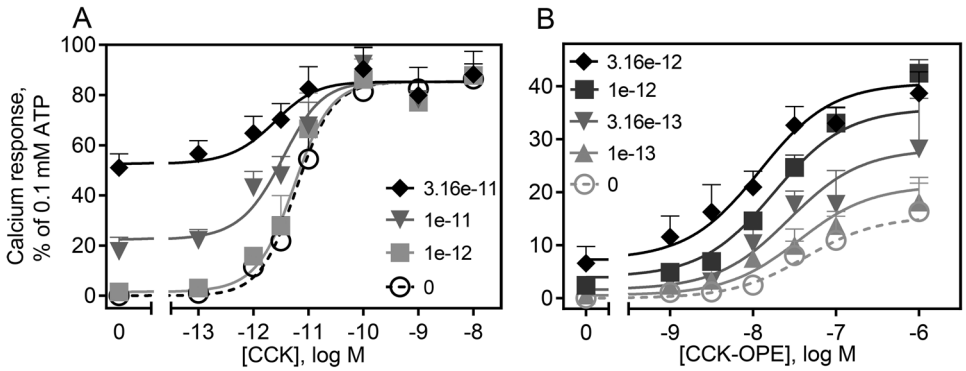

Molecular Pharmacology Fast Forward. Published on December 27, 2018 as DOI: 10.1124/mol.118.114082
This article has not been copyedited and formatted. The final version may differ from this version.

Figure 3

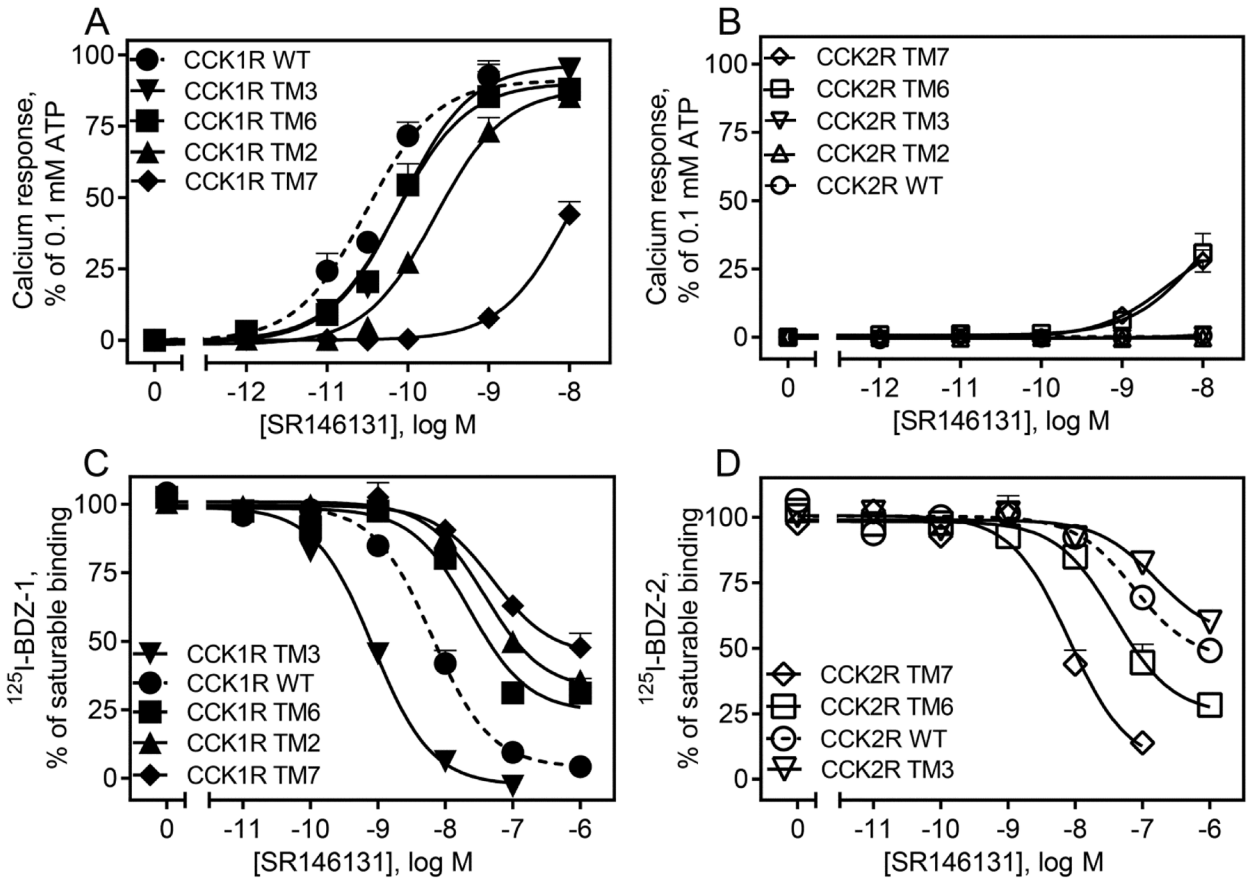

Molecular Pharmacology Fast Forward. Published on December 27, 2018 as DOI: 10.1124/mol.118.114082
This article has not been copyedited and formatted. The final version may differ from this version.

Figure 4

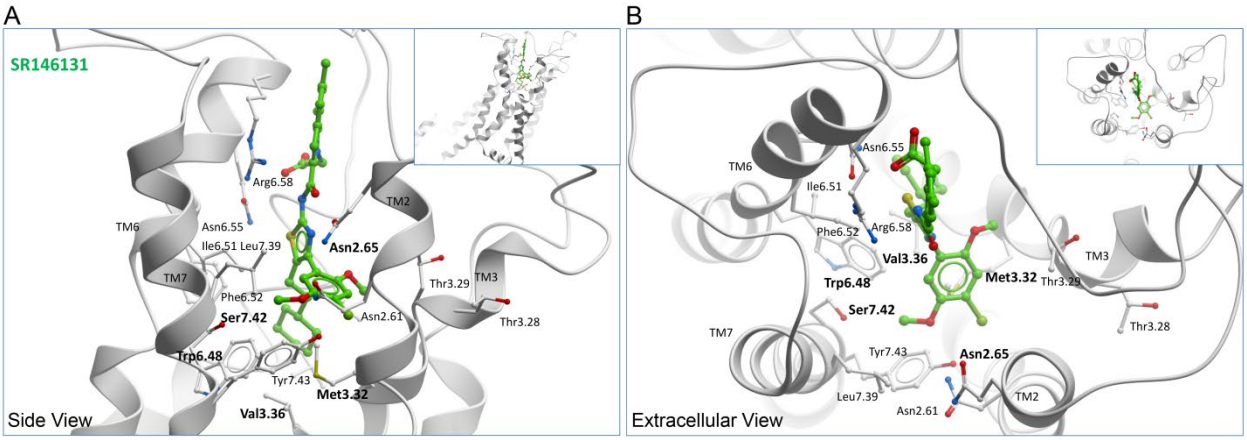

Molecular Pharmacology Fast Forward. Published on December 27, 2018 as DOI: 10.1124/mol.118.114082
This article has not been copyedited and formatted. The final version may differ from this version.

Figure 5

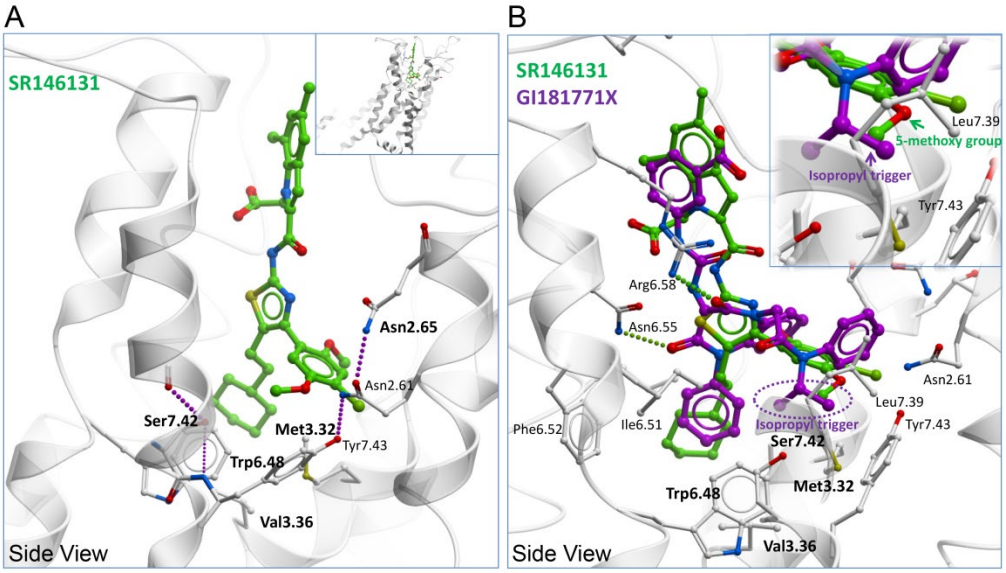

Molecular Pharmacology Fast Forward. Published on December 27, 2018 as DOI: 10.1124/mol.118.114082
This article has not been copyedited and formatted. The final version may differ from this version.

Figure 6

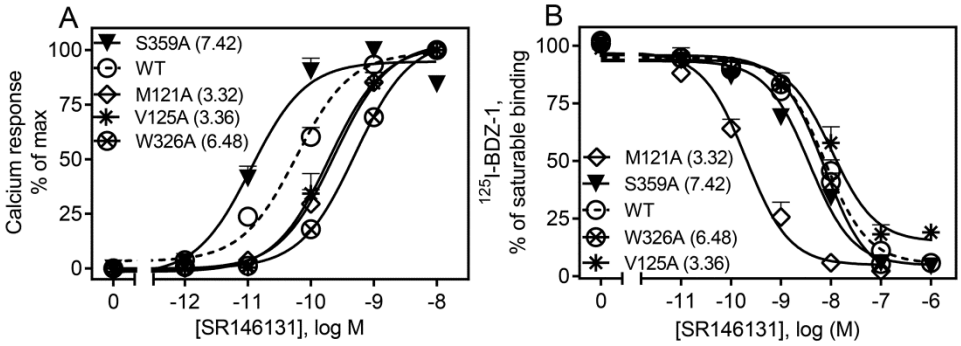

Molecular Pharmacology Fast Forward. Published on December 27, 2018 as DOI: 10.1124/mol.118.114082
This article has not been copyedited and formatted. The final version may differ from this version.

Figure 7

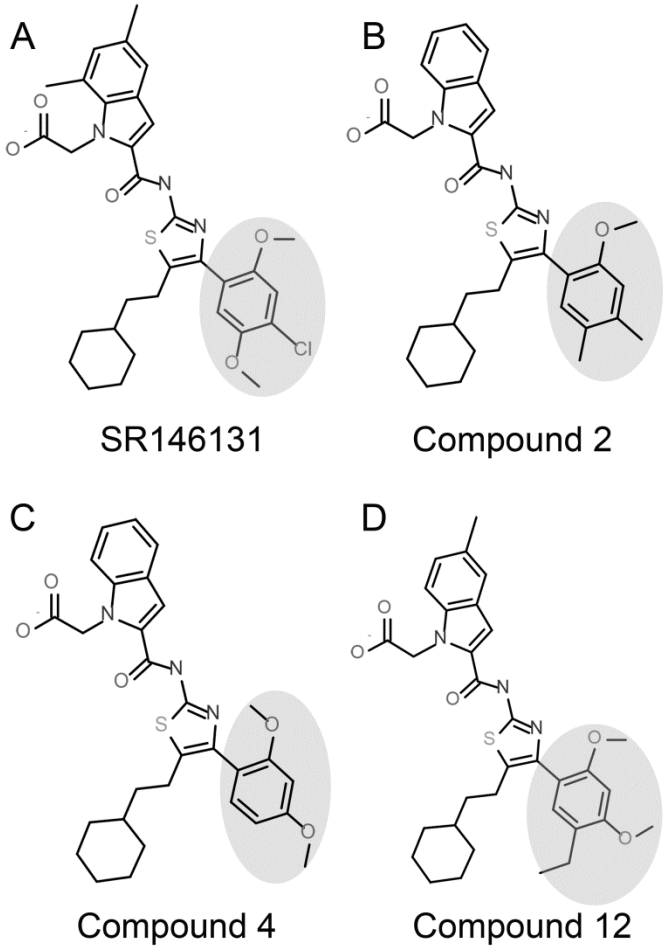

Molecular Pharmacology Fast Forward. Published on December 27, 2018 as DOI: 10.1124/mol.118.114082
This article has not been copyedited and formatted. The final version may differ from this version.

Figure 8

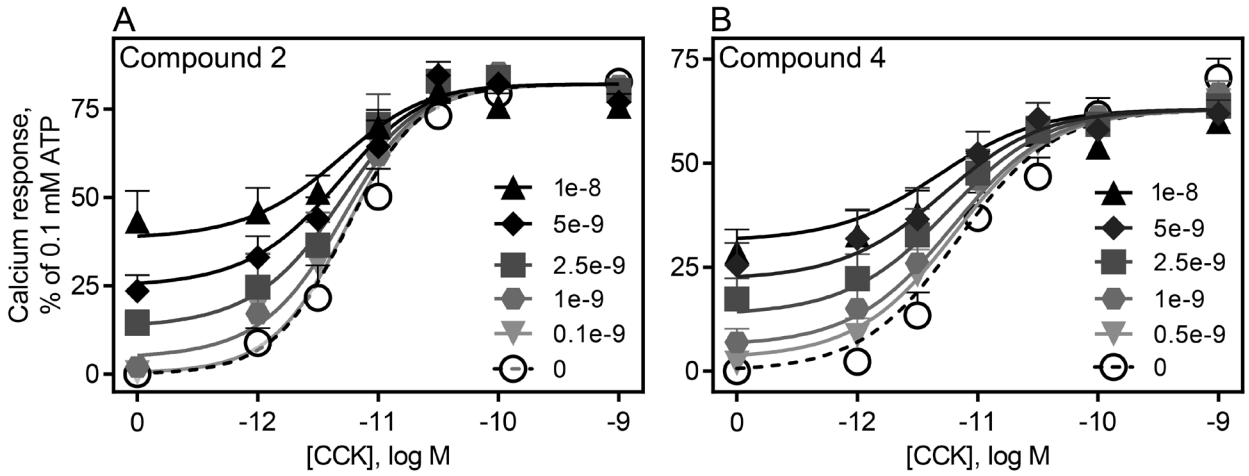

Molecular Pharmacology Fast Forward. Published on December 27, 2018 as DOI: 10.1124/mol.118.114082
This article has not been copyedited and formatted. The final version may differ from this version.

Figure 9

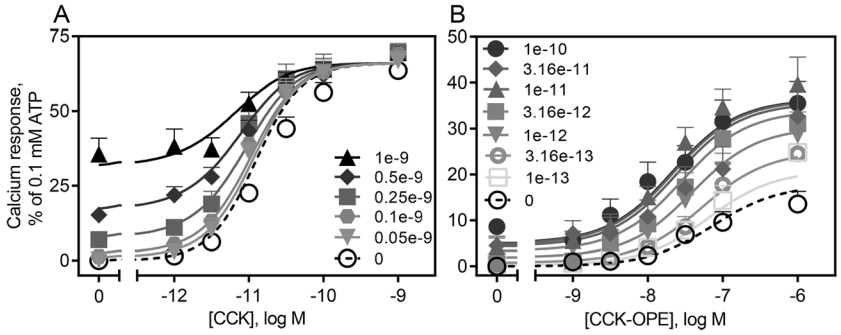

Molecular Pharmacology Fast Forward. Published on December 27, 2018 as DOI: 10.1124/mol.118.114082
This article has not been copyedited and formatted. The final version may differ from this version.

Figure 10

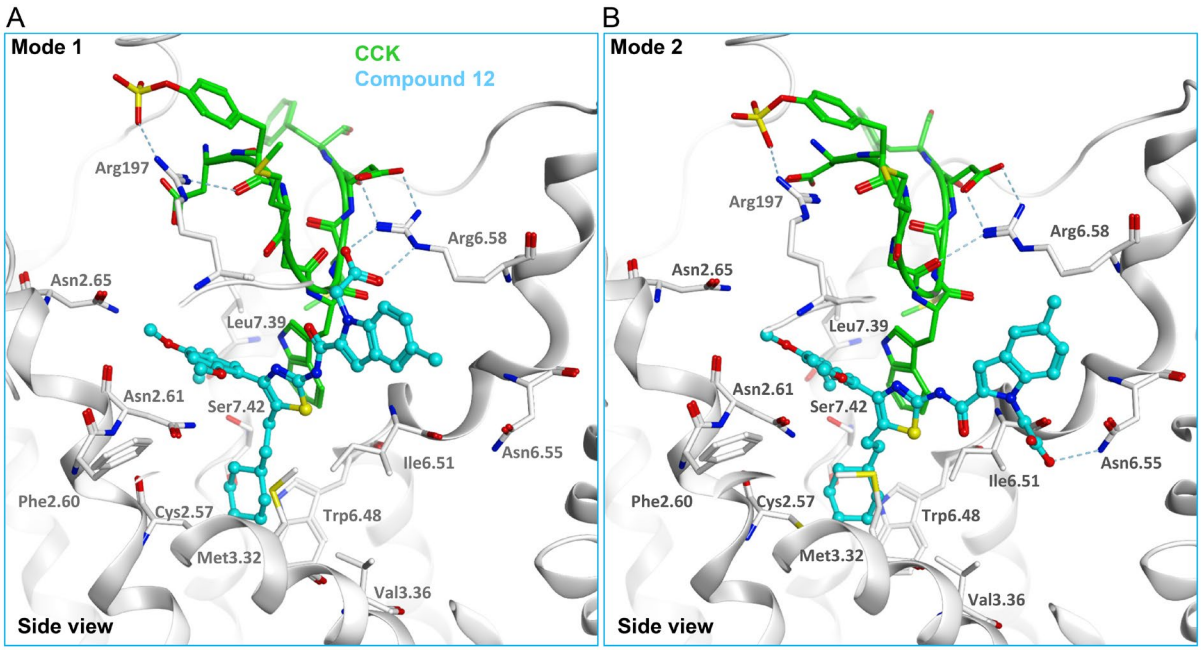

Molecular Pharmacology Fast Forward. Published on December 27, 2018 as DOI: 10.1124/mol.118.114082
This article has not been copyedited and formatted. The final version may differ from this version.

Figure 11

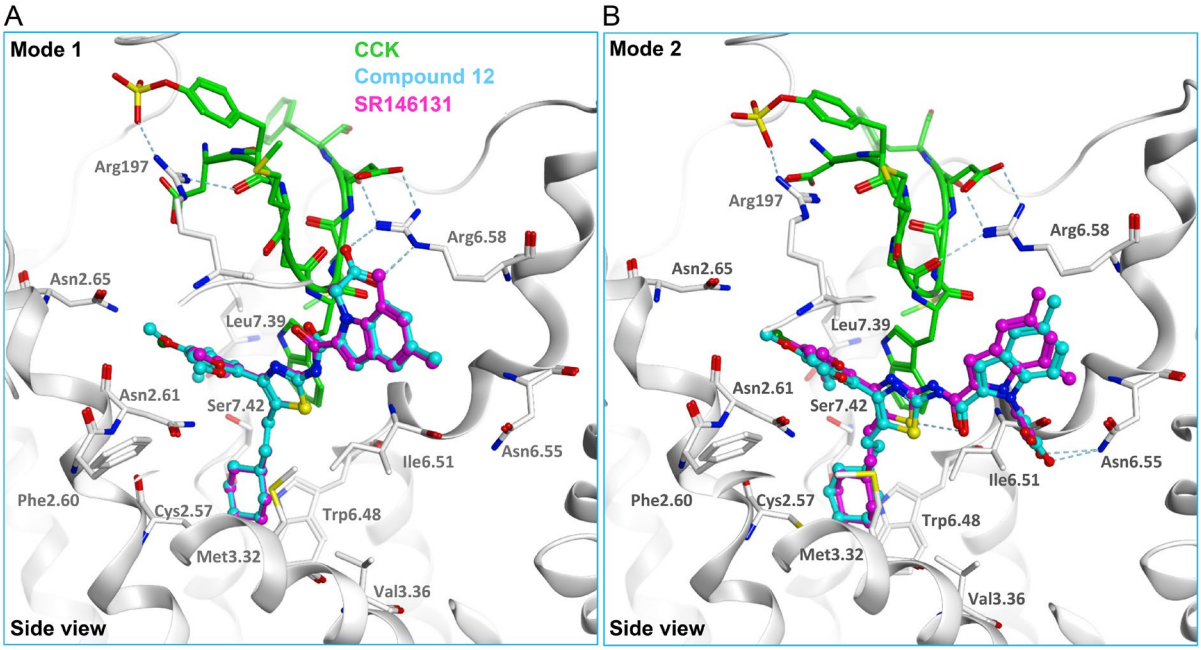

Molecular Pharmacology Fast Forward. Published on December 27, 2018 as DOI: 10.1124/mol.118.114082
This article has not been copyedited and formatted. The final version may differ from this version.

Figure 12

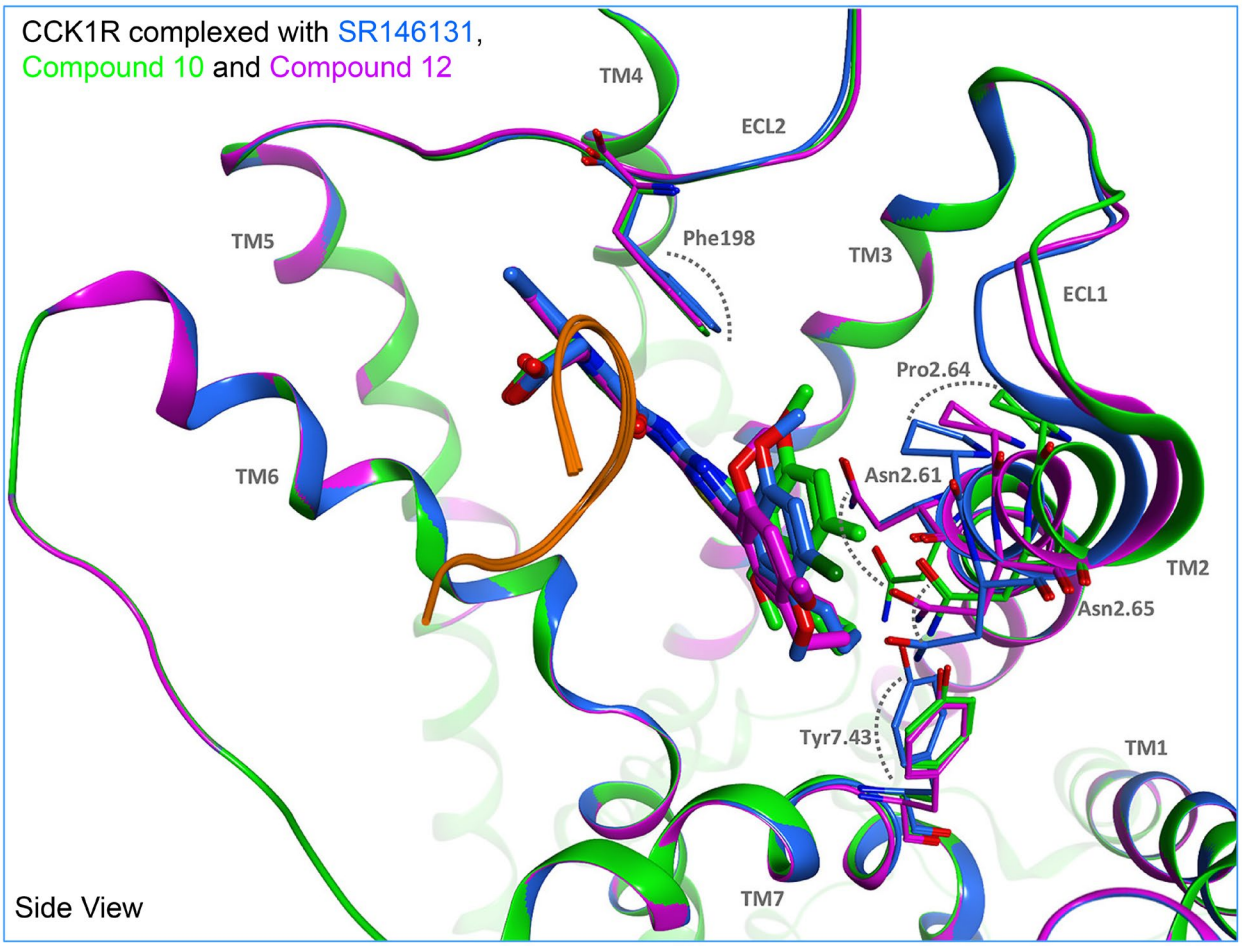

Molecular Pharmacology Fast Forward. Published on December 27, 2018 as DOI: 10.1124/mol.118.114082
This article has not been copyedited and formatted. The final version may differ from this version.

Figure 13